Am J Cancer Res 2024;14(4):1523-1544
www.ajcr.us /ISSN:2156-6976/ajcr0154411

Original Article

FAT10 mediates the sorafenib-resistance of hepatocellular carcinoma cells by stabilizing E3 ligase NEDD4 to enhance PTEN/AKT pathway-induced autophagy

Wenming Zhang[1,2,3,4], Dongnian Du[1,2,3,4], Hongcheng Lu[1,2,3,4], Dandan Zhang[1,2,3,4], Lingpeng Liu[1,2,3,4], Jiajuan Li[1,2,3,4], Zehao Chen[1,2,3,4], Xuzhe Yu[1,2,3,4], Miao Ye[1,2,3,4], Wei Wang[1,2,3,4], Leifeng Chen[1,2,3,4], Jianghua Shao[1,2,3,4]

[1]Department of General Surgery, The Second Affiliated Hospital of Nanchang University, Nanchang 330000, Jiangxi, China; [2]Jiangxi Province Key Laboratory of Molecular Medicine, The Second Affiliated Hospital of Nanchang University, Nanchang 330000, Jiangxi, China; [3]Liver Cancer Institute, Nanchang University, Nanchang 330000, Jiangxi, China; [4]Jiangxi Province Clinical Research Center of General Surgery, The Second Affiliated Hospital of Nanchang University, Nanchang 330000, Jiangxi, China

Received November 14, 2023; Accepted March 31, 2024; Epub April 15, 2024; Published April 30, 2024

Abstract: Although sorafenib is the first-line therapeutic agent for advanced hepatocellular carcinoma (HCC), the development of drug resistance in HCC cells limits its clinical efficacy. However, the key factors involved in mediating the sorafenib resistance of HCC cells and the underlying mechanisms have not been elucidated. In this study, we generated sorafenib-resistant HCC cell lines, and our data demonstrate that HLA-F locus-adjacent transcript 10 (FAT10), a ubiquitin-like protein, is markedly upregulated in sorafenib-resistant HCC cells and that reducing the expression of FAT10 in sorafenib-resistant HCC cells increases sensitivity to sorafenib. Mechanistically, FAT10 stabilizes the expression of the PTEN-specific E3 ubiquitin ligase NEDD4 that causes downregulation of PTEN, thereby inducing AKT-mediated autophagy and promoting the resistance of HCC cells to sorafenib. Moreover, we screened the small molecule Compound 7695-0983, which increases the sensitivity of sorafenib-resistant HCC cells to sorafenib by inhibiting the expression of FAT10 to inhibit NEDD4-PTEN/AKT axis-mediated autophagy. Collectively, our preclinical findings identify FAT10 as a key factor in the sorafenib resistance of HCC cells and elucidate its underlying mechanism. This study provides new mechanistic insight for the exploitation of novel sorafenib-based tyrosine kinase inhibitor (TKI)-targeted drugs for treating advanced HCC.

Keywords: Sorafenib resistance, FAT10, E3 ligase NEDD4, autophagy, hepatocellular carcinoma cells

Introduction

Autophagy is an evolutionarily conserved catabolic degradation process in cells in which cytoplasmic components are captured by double-membrane vesicles (autophagosomes) and delivered to lysosomes for degradation and final recycling. Autophagy is a vital mechanism for maintaining cellular homeostasis [1]. Increasing evidence has highlighted that abnormal regulation of autophagy is closely correlated with the occurrence and development of various diseases, including cancers [2, 3]. Enhanced autophagy in tumor cells can help cells resist stress and survive, thereby promoting the malignant progression of tumors [4, 5]. In addition, studies have suggested that autophagy is strongly correlated with drug resistance in tumors [6, 7]. Autophagy functions as a protective mechanism for cancer cells that have been exposed to numerous anticancer drugs. When autophagy in tumor cells is inhibited, this can prevent the development of tumor drug resistance and improve the effect of antitumor therapy [8]. In recent years, autophagy has attracted attention respect of in drug resistance to sorafenib, which is the first FDA-approved first-line systemic drug for treating advanced hepatocellular carcinoma (HCC) [9, 10]. Studies have revealed that autophagy is

https://doi.org/10.62347/EPIT4481

abnormally elevated in sorafenib-resistant HCC cells, and inhibition of autophagy can enhance the response of sorafenib-resistant HCC cells to treatment with sorafenib [11-13]. However, the mechanism by which autophagy mediates sorafenib resistance in HCC cells is complex and requires further exploration.

HLA-F locus-adjacent transcript 10 (FAT10) is a specific ubiquitin-like protein, which can directly mediate the ubiquitin-independent proteasomal degradation of substrates [14]. FAT10 is involved in the regulation of cellular biological processes such as cellular immunity, apoptosis, signal transduction and the cell cycle [15]. The expression of FAT10 is upregulated in various cancers [16]. Our previous research confirmed that FAT10 can compete with ubiquitin (Ub) to form a FAT10 substrate complex, and the FAT10 substrate complex is not degraded by the proteasome, thus stabilizing the expression of substrate proteins and promoting tumor progression [17-20]. We also found that FAT10 can stabilize and degrade substrates in HCC cells simultaneously [21]. In addition, our latest research showed that FAT10 can stabilize multiple substrates by antagonizing their ubiquitination in HCC cells simultaneously [22]. However, whether FAT10 is involved in mediating sorafenib resistance of HCC cells by exerting the function of stabilizing substrate remains unclear.

Neuronal precursor cell-expressed developmentally downregulated 4 (NEDD4) is prominent member of the highly conserved homologous E6-AP carboxyl terminus (HECT) domain E3 ligase family in eukaryotes [23]. The E3 ubiquitin ligase NEDD4 exerts its biological function by interacting with different target proteins and promoting the ubiquitination of substrates [24, 25]. In recent years, NEDD4 has been shown to play a major role in affecting the development of tumors [26-28]. In addition, studies have also showed that NEDD4, as a specific E3 ubiquitin ligase of phosphatase and tensin homolog (PTEN), can inhibit PTEN protein expression by promoting its polyubiquitination and subsequent proteasomal degradation [29, 30]. The PTEN-mediated AKT signaling pathway is abnormally activated and the autophagy level was significantly increased in sorafenib-resistant HCC cells, and PTEN-mediated inhibition of the AKT signaling pathway can significantly increase the sensitivity of sorafenib-resistant HCC cells to sorafenib [31]. Therefore, based on the fact that NEDD4 can regulate PTEN expression and the importance of PTEN/AKT signaling pathway-mediated autophagy in promoting sorafenib resistance, we hypothesize that FAT10 could stabilize NEDD4 expression, which in turn downregulates PTEN expression to enhance AKT signaling pathway-mediated autophagy, thereby facilitating sorafenib resistance in HCC cells.

In this study, by generating sorafenib-resistant HCC cell lines, our results showed that FAT10 expression was significantly upregulated in sorafenib-resistant cell lines and that knockdown FAT10 expression in sorafenib-resistant cells could increase sensitivity to sorafenib treatment. Mechanistic studies have shown that FAT10 increases the autophagy level of HCC cells by stabilizing the expression of the NEDD4 to downregulate PTEN expression and activate the AKT signaling pathway, thereby facilitating the resistance of HCC cells to sorafenib. Finally, we screened the small molecule Compound 7695-0983, which can inhibit the expression of FAT10, thereby enhancing the sensitivity of sorafenib-resistant HCC cells to sorafenib treatment.

Materials and methods

Cell culture and reagents

Human HCC cell lines (Huh7 and HepG2 cells) were obtained from the National Collections of Authenticated Cell Cultures, Chinese Academy of Sciences. To establish sorafenib-resistant clones, Huh7 and HepG2 cells were successively treated with increasing concentrations of sorafenib, followed by training treatment with 5.5 μM sorafenib. Cells were cultured in Dulbecco's modified Eagle's medium (Gibco) supplemented with antibiotics and 10% fetal bovine serum (Gibco) at 37°C and 5% CO_2. Sorafenib, rapamycin and SC79 were purchased from MedChemExpress (Monmouth Junction, NJ, USA).

Cell transfection

The FAT10-overexpressing and shFAT10-expressing plasmids were purchased from Genechem (Shanghai, China). Transfection was carried out in 60-70% confluent cells by apply-

ing Lipofectamine 3000 reagent according to the manufacturer's protocol. Huh7 and HepG2 cell lines stably expressing FAT10 plasmids and Huh7 and HepG2 cell lines stably expressing shFAT10 plasmids were screened for 4 weeks with puromycin (2.5 μg/mL). The shRNAs targeting FAT10 sequences: 5'-GGAGAAGCCTCTCATCTTA-3' (shFAT10#1) and 5'-GGCAGATTACGGCATCAGA-3' (shFAT10#2).

Clinical HCC specimens

A total of 14 human liver puncture biopsy samples, which were obtained from patients with a clinical and histopathological HCC diagnosis and treated with sorafenib, were collected from the Second Affiliated Hospital of Nanchang University. Informed consent was obtained from each patient and the study protocol was approved by the ethics committee of the second affiliated hospital of Nanchang University.

Western blotting

Western blotting was performed as described previously [22]. These primary antibodies were applied to the Western blotting: anti-FAT10 (1:500, MABS351, Merck Millipore, Billerica, MA, USA and PA5-72864, Invitrogen, MA, USA), anti-NEDD4 (1:1000, 21698-1-AP, Proteintech, China), anti-PTEN (1:1000, ab267787, Abcam, USA), anti-p-AKT (1:1000, ab18206, Abcam, USA), anti-AKT (1:1000, ab8805, Abcam, USA), anti-MAP1LC3B (1:1000, ab192890, Abcam, USA), anti-Caspase3 (1:1000, ab32351, Abcam, USA), and anti-cleaved PARP1 (1:1000, 13371-1-AP, Proteintech, China) antibodies. The membrane was incubated with horseradish peroxidase-conjugated goat anti-rabbit or anti-mouse IgG secondary antibodies (1:5000, Abcam) for 60 min at room temperature (RT). Immunoreactive signals were developed using chemiluminescence.

Flow cytometry analysis

Cell apoptosis was detected using a FITC Annexin V Apoptosis Detection Kit (BD Biosciences) according to the protocol of manufacturer. Cells were collected and resuspended in ice-cold PBS, followed by staining with 5% Annexin V-FITC and 5% propidium iodide (PI) for 15 min at RT in the darkness. Samples were detected utilizing a FACSCalibur flow cytometer (BD Biosciences, USA), and the data were analyzed using FlowJo software version 10.

Immunohistochemical (IHC) analysis

Tumor tissue sections were dehydrated with a graded alcohol series, cleared with xylene, and subjected to antigen retrieval with citrate buffer (0.01 M). The sections were blocked using protein blocking buffer without serum for 30 min, followed by incubation with anti-FAT10 (1:500, MA5-32487, Invitrogen), anti-NEDD4 (1:1000, 21698-1-AP, Proteintech, China) and anti-MAP1LC3 (1:1000, PA1-16930, Invitrogen) antibodies. Images of the sections were captured under an Olympus BH-2 microscope (Olympus). The 3,3'-diaminobenzidine signal was quantified using ImageJ v.1.51 (National Institutes of Health).

RNA extraction and quantitative real-time polymerase chain reaction (qRT-PCR)

Extraction of total RNA from the cultured cells using TRIzol reagent (Invitrogen, 15596026) following the instructions of manufacturer. The isolated RNA was reverse-transcribed into complementary DNA (cDNA) with the PrimeScript RT reagent kit (RR036A, Takara, Japan). The cDNA was subjected to qRT-PCR analysis with TB Green® Fast qPCR Mix (RR430A, Takara, Japan) and a QuantStudio5 Q5 (Applied Biosystems). The primers sequences utilized for qRT-PCR assay were as below: FAT10, 5'-CTCTGGTTTCTGGCCCCTTG-3' (forward) and 5'-CCATTCCTCGGAACGGACAT-3' (reverse); NEDD4, 5'-GTGCAGACTCACCTTGCAGA-3' (forward) and 5'-TTTTTCTTCCCAACCTGGTG-3' (reverse); and GAPDH, 5'-CATACCAGGAAATGAGCTTGAC-3' (forward) and 5'-AACAGCGACACCCACTCCTC-3' (reverse).

Subcutaneous xenograft transplantation

A subcutaneous xenograft transplantation mouse model was established to examine the tumorigenic capacity of FAT10 knockdown HCC cells treated with sorafenib. Male athymic BALB/c nude mice aged 6-8 weeks were procured from Gempharmatech Co., Ltd. shNC Huh7-SR, shFAT10 Huh7-SR cells, shNC HepG2-SR and shFAT10 HepG2-SR cells stably transduced with firefly luciferase gene. 100 μL of phosphate-buffered saline (PBS) which containing 1×10^7 cells were injected subcutane-

ously into the flanks of nude mice. After 1 week, the mice in the experimental groups were intraperitoneally injected with sorafenib (30 mg/kg bodyweight) twice a week. The width and length of the tumors were determined once every five days with Vernier calipers. The tumor volume (V) was measured as follows: $V = 0.52 \times \text{length} \times \text{width}^2$. For the detection of bioluminescent signals in vivo, mice were anesthetized utilizing isoflurane and subsequently imaged on a Lumina Series III IVIS (In Vivo Imaging System) instrument (PerkinElmer, MA, USA). After the observation period, the mice were euthanized. The tumors were excised and imaged.

Coimmunoprecipitation (Co-IP)

Coimmunoprecipitation was performed as described previously [22]. Cells were lysed in the cell lysis buffer for IP and Western (Beyotime Biotechnology, 50 mM Tris·HCl, pH 8.0, 0.5% Nonidet P-40, 5 mM EDTA, and 150 mM NaCl) and centrifuged at 16,000 × g for 15 minutes for debris removal. Cleared lysates were immunoprecipitated utilizing antibodies. Roll overnight at 4°C. Protein A/G PLUS-agarose (Santa Cruz Biotechnology, USA) was thereafter added and rolling was continued for 8 hours. Cleaning three times with Wash Buffer. Western blot and SDS-PAGE were later implemented with proper Bis-Tris Gel.

In vivo ubiquitination assay

Cells were exposed to 15 mmol/L MG132 for eight hours, and subsequently cell lysates were immunoprecipitated by anti-NEDD4 antibody. NEDD4 ubiquitination was examined with anti-ubiquitin antibody.

Terminal deoxynucleotidyl transferase dUTP nick end labeling (TUNEL) assay

Apoptosis was investigated by TUNEL assay utilizing an in situ cell death detection kit (Roche, Indianapolis, IN, USA) in accordance with the instructions of the manufacturer. To gain quantitative results, TUNEL-positive cells were countered in five random area images for each sample with ImageJ.

Liquid chromatography-tandem mass spectrometry (LC-MS/MS) analysis

FAT10 was immunoprecipitated from the lysates of HCC cells using the same protocols as those used for the co-IP assay. Samples were cultured in electrophoresis sample buffer and underwent electrophoresis on sodium dodecyl sulfate-polyacrylamide gels. The gel was stained via utilizing Coomassie brilliant blue for 3 hours and cleaned utilizing an eluent overnight. The proteins resolved from the gels were analyzed by LC-MS/MS as described previously [32].

Molecular docking analysis

The structure of proteins and compounds were optimized for docking analysis using the Discovery Studio (DS) 2019 Client. The hydrogenation and force field structure were optimized by removing water molecules from the NEDD4 (PDB ID: 5C91) and FAT10 (PDB ID: 6GF2) receptor model structures. The ZDOCK module of DS software was used to dock the protein receptor and ligand in an induced-fit method. The cavity of 20 Å was selected as the docking active region, and the docking calculation was carried out with standard parameters. The docking models with the highest score were analyzed and visualized.

Generation of CRISPR-Cas9 knockout cell lines

To establish Huh7 and HepG2 cells deficient in FAT10, we designed the specific target sequences for single-guide RNA synthesis, the primer sequences (5' to 3') were: FAT10#1 forward cacc gcatgtccgttccgaggaat, reverse aaac attcctcggaacggacatgc; FAT10#2 forward cacc gcaatgatcgagactaagac, reverse aaac gtcttagtctcgatcattgc. Pairs of annealed oligos were ligated into the pX459 (Addgene Plasmid #48139) after being digested with BbsI (Thermo). The cells were transfected with 2 μg of total plasmid DNA per well in 6-well plates using Lipofectamine 3000 (Invitrogen) according to the manufacturer's instructions. After 2 days, these cells were treated with 1 μg/mL puromycin for 72 h for enrichment. The surviving cells were sorted into single clones in a 96-well plate. The viable clones further grown for approximately one week, and 80% of the cells per well were picked up for DNA isolation and genotyping. The genomic PCR primer sequences (5' to 3') for genotyping $FAT10^{-/-}$ cells were: reverse ctagaggaccagatagatag, forward cctccaatacaataacatgc. The remaining 20% of the cells were cultured for 8-10 days, and clones propagated from single cells were

picked out. The knockout efficacy of FAT10$^{-/-}$ cells was confirmed by both western blotting.

Statistical analysis

All statistical analyses were performed using GraphPad Prism 9.0. Data are presented as the mean ± SD. Differences between two groups were analyzed using Student's t test; differences between more than two groups were analyzed by one-way analysis of variance (ANOVA). All experiments were independently repeated three times. Differences were considered significant at $P < 0.05$.

Results

Reducing the expression of FAT10 in HCC-SR cells enhances sorafenib-induced apoptosis in vitro and in vivo

To investigate whether FAT10 in HCC cells is involved in sorafenib resistance, we established two sorafenib-resistant (SR) HCC cell lines in HepG2 and Huh7 cells (HepG2-SR and Huh7-SR) (Figure S1A and S1B). The qRT-PCR and Western blot results showed that compared with those in the parental HCC cell lines, the expression levels of FAT10 mRNA and protein were upregulated in HCC-SR cells (**Figures 1A**, S2A). Furthermore, we knocked down FAT10 in HepG2-SR and Huh7-SR cells with shRNA (shFAT10 HepG2-SR and shFAT10 Huh7-SR), and the qRT-PCR and Western blot results showed that compared with shNC HCC-SR cells, the expression of FAT10 mRNA and protein in shFAT10 HCC-SR cells was significantly reduced (**Figures 1B**, S2B). Sorafenib was used to treat HCC-SR cells in the shNC and shFAT10 groups, and apoptosis was detected via flow cytometry and TUNEL assays. The results showed that compared with shNC HCC-SR cells, the apoptosis rate of shFAT10 HCC-SR cells in response to sorafenib was significantly increased (**Figures 1C**, **1D**, S2C, S2D). Moreover, the Western blot results showed that compared with shNC HCC-SR cells, the protein expression levels of the apoptosis-related proteins cleaved Caspase3 and cleaved PARP1 in shFAT10 HCC-SR cells were significantly increased (**Figures 1E**, S2E). Overall, our results indicate that reducing the expression of FAT10 in HCC-SR cell lines can increase sorafenib-induced apoptosis in vitro.

Our in vivo data also confirmed that knocking down the expression of FAT10 in HCC-SR cells could increase the apoptosis induced by sorafenib. We constructed subcutaneous tumor-bearing models of nude mice using shNC HCC-SR cells and shFAT10 HCC-SR cells, which were then treated with sorafenib. Evaluation of the subcutaneous tumor-bearing model in HCC-SR cells using an in vivo fluorescence imaging system (IVIS) revealed that compared with the shNC group, the tumor volume of the shFAT10 group was significantly decreased after sorafenib treatment (**Figures 1F**, S2F). Statistical analysis showed that compared with the shNC HCC-SR cells, the shFAT10 HCC-SR cells had a slower growth rate and significantly reduced tumor weight (**Figures 1G**, **1H**, S2G, S2H). IHC and fluorescence analysis of tumor tissues showed that compared with the corresponding shNC group, the expression of FAT10 in the tumor tissues of the shFAT10 group was significantly decreased, and the apoptosis rate was significantly increased (**Figures 1I**, S2I). In addition, our results also found that reducing the expression of FAT10 significantly increased sorafenib-induced apoptosis; however, overexpression of FAT10 could attenuate sorafenib-induced apoptosis (Figure S3A-D). Taken together, our results suggest that reducing the expression of FAT10 in HCC-SR cells could significantly increase their sensitivity to sorafenib treatment in vitro and in vivo.

Knockdown of FAT10 expression promotes sorafenib-induced apoptosis by inhibiting autophagy in HCC-SR cells

Studies have highlighted the important role that autophagy plays in sorafenib resistance [33, 34]. Therefore, we wanted to further explore whether reducing the expression of FAT10 in HCC-SR cells increases the sensitivity to sorafenib by affecting autophagy. Our result first found that compared with those in the parental HCC cell lines, the expression level of autophagy-related protein LC3-II were upregulated in HCC-SR cells (**Figure 2A**). Furthermore, Western blot analysis revealed that compared with the shNC HCC-SR cells, the expression level of LC3-II protein decreased in the shFAT10 HCC-SR cells (**Figure 2B**). Moreover, we constructed an mRFP-GFP-LC3 reporter, and the results showed that compared with that in shNC HCC-SR cells, the level of autophagy in

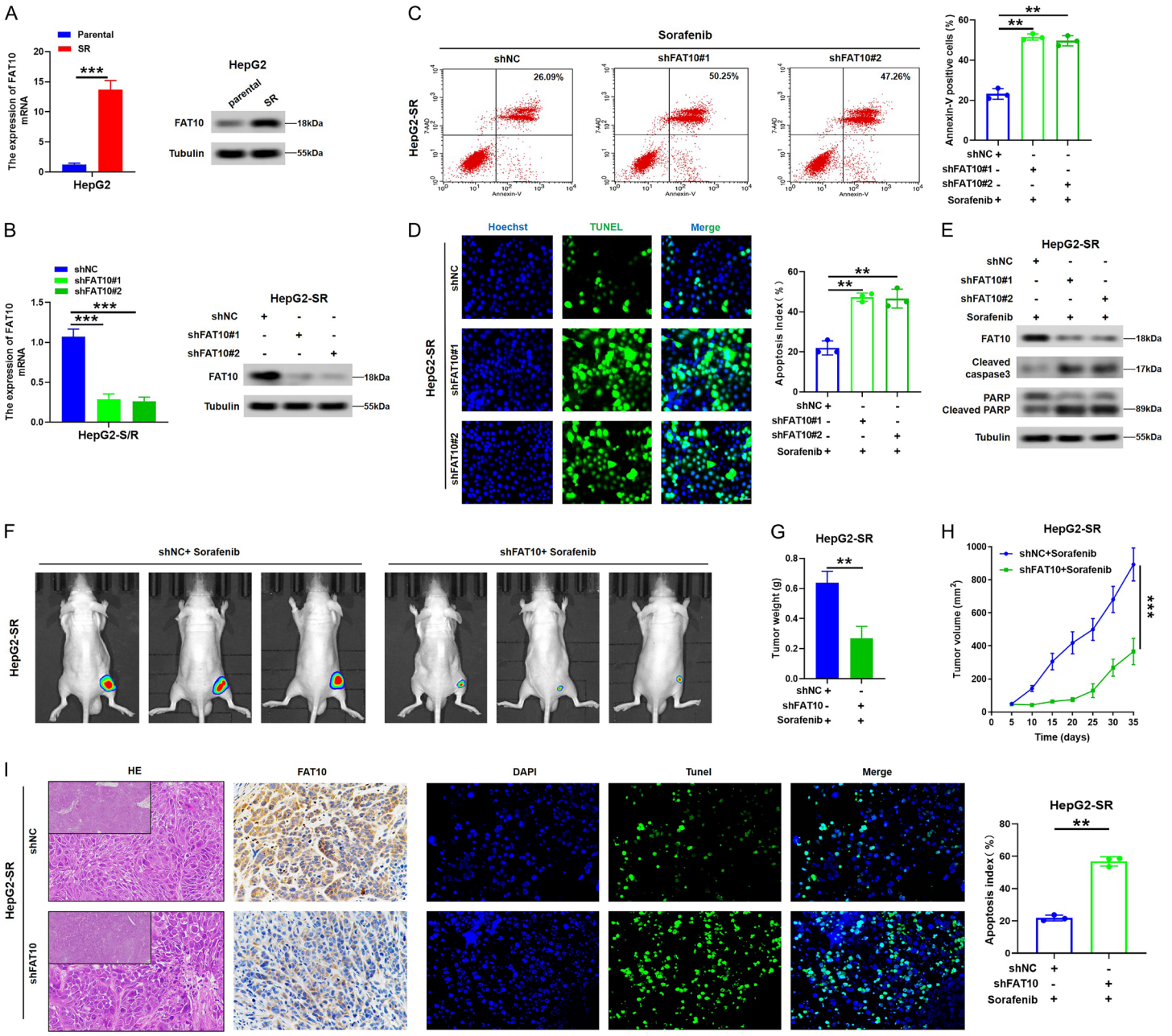
A
Parental
SR
The expression of FAT10 mRNA
HepG2
HepG2
parental
SR
FAT10
18kDa
Tubulin
55kDa
B
shNC
shFAT10#1
shFAT10#2
The expression of FAT10 mRNA
HepG2-S/R
HepG2-SR
shNC
shFAT10#1
shFAT10#2
FAT10
18kDa
Tubulin
55kDa
C
Sorafenib
shNC
shFAT10#1
shFAT10#2
HepG2-SR
26.09%
50.25%
47.26%
Annexin-V positive cells (%)
shNC
shFAT10#1
shFAT10#2
Sorafenib
D
Hoechst
TUNEL
Merge
HepG2-SR
shNC
shFAT10#1
shFAT10#2
Apoptosis index (%)
E
HepG2-SR
shNC
shFAT10#1
shFAT10#2
Sorafenib
FAT10
18kDa
Cleaved caspase3
17kDa
PARP
Cleaved PARP
89kDa
Tubulin
55kDa
F
shNC+ Sorafenib
shFAT10+ Sorafenib
HepG2-SR
G
HepG2-SR
Tumor weight (g)
shNC
shFAT10
Sorafenib
H
HepG2-SR
shNC+Sorafenib
shFAT10+Sorafenib
Tumor volume (mm3)
Time (days)
I
HE
FAT10
DAPI
Tunel
Merge
HepG2-SR
shNC
shFAT10
HepG2-SR
Apoptosis index (%)
shNC
shFAT10
Sorafenib

Figure 1. Reducing the expression of FAT10 in HCC-SR cells enhances sorafenib-induced apoptosis in vitro and in vivo. (A) qRT-PCR analysis and Western blot analysis of FAT10 expression in parental and HepG2-SR cells. (B) qRT-PCR analysis and Western blot analysis of FAT10 expression in FAT10-knockdown HepG2-SR cells. (C) Flow cytometry analysis of apoptosis in shNC- or shFAT10-transfected HepG2-SR cells (10 μM) after exposure to sorafenib for 24 h. (D) Representative figures and quantification of TUNEL staining showing apoptotic cells (stained in green). (E) Western blot analysis of the expression of cleaved caspase, PARP, and cleaved PARP in shNC- or shFAT10-transfected HepG2-SR cells after exposure to sorafenib for 24 h. (F) Nude mice injected with luciferase-expressing shNC or shFAT10 HepG2-SR cells were treated with sorafenib (30 mg/kg/day) intraperitoneally, and then subcutaneous xenografts were assessed by an IVIS imaging system (n = 6). (G and H) The (G) weights and (H) volumes of subcutaneous tumors were measured. (I) IHC detected the expression of FAT10 in subcutaneous xenografts and representative figures of TUNEL staining showing apoptotic cells (stained in green) in subcutaneous xenografts. Scale bars: 100 μm. $^{**}P < 0.01$, $^{***}P < 0.001$.

shFAT10 HCC-SR cells was also significantly inhibited (**Figure 2C**). Similar experimental results were obtained using transmission electron microscopy analysis (**Figure 2D**). In addition, IHC analysis was used to determine the expression of LC3-II protein in subcutaneous tumor-bearing tissues of nude mice. The results showed that compared with that in the shNC group, the expression of LC3-II in the shFAT10 group was significantly decreased (**Figure 2E**). Thus, these results suggest that knockdown of FAT10 expression can inhibit autophagy in HCC-SR cells. Next, we knocked down FAT10 expression in HCC-SR cells and treated them with the autophagy agonist rapamycin. The results showed that FAT10 knockdown suppressed autophagy and increased sorafenib-induced apoptosis in HCC-SR cells; however, rapamycin mitigated the effects of FAT10 knockdown on autophagy and sorafenib-induced apoptosis (**Figure 2F-I**). Taken together, our data indicate that knockdown of FAT10 in HCC-SR cells enhances their sensitivity to sorafenib by inhibiting autophagy.

Downregulation of FAT10 promotes sorafenib-induced apoptosis by upregulating PTEN to inhibit AKT pathway-mediated autophagy in HCC-SR cells

The Cancer Genome Atlas dataset was subjected to gene set enrichment analysis to investigate the potential correlation between FAT10 and various signaling pathways. As shown in **Figure 3A**, the PI3K/AKT/mTOR pathway was markedly enriched in HCC samples exhibiting FAT10 upregulation, suggesting that the PI3K/AKT/mTOR pathway was strongly correlated with the upregulation of FAT10 in HCC. Studies have con-firmed that the PTEN/AKT signaling pathway is closely related to autophagy [35, 36]. Therefore, we aimed to further investigate whether FAT10 affects the sensitivity of HCC-SR cells to sorafenib by upregulating PTEN to inhibit AKT pathway-mediated autophagy. To this end, we analyzed the correlation between the expression of FAT10 and PTEN/AKT pathway-related proteins in shNC HCC-SR cells and shFAT10 HCC-SR cells. The Western blot results showed that compared with the shNC HCC-SR cells, the expression of PTEN increased in the shFAT10 HCC-SR cells, while the expression levels of phosphorylated AKT (p-AKT) was decreased (**Figure 3B**). Next, we treated shFAT10 HCC-SR cells with the specific AKT signaling activator SC79. The results showed that SC79 inhibited FAT10 knockdown-induced upregulation of PTEN expression, the inhibition of autophagy mediated by the AKT pathway and upregulation of sorafenib-induced apoptosis in HCC-SR cells (**Figure 3C-F**). Taken together, our data indicate that knockdown of FAT10 in HCC-SR cells enhances their sensitivity to sorafenib by upregulating PTEN to inhibit AKT-pathway-mediated autophagy.

Downregulation of FAT10 promotes sorafenib-induced apoptosis by inhibiting the NEDD4-mediated PTEN/AKT pathway in HCC-SR cells

Studies have highlighted that NEDD4 is a specific E3 ubiquitin ligase of PTEN and plays an important role in regulating the expression of the PTEN protein [29]. On this basis, we sought to explore whether FAT10 regulates PTEN/AKT-mediated autophagy by regulating NEDD4 in HCC-SR cells, thereby affecting their sensitivity to sorafenib. Thus, we further investigated the expression of NEDD4 in parental HCC cells and HCC-SR cells. Western blot results showed that compared with those in the parent HCC cell lines, the expression levels of NEDD4 were upregulated in the HCC-SR lines (**Figure 4A**). Furthermore, we determined the expression of

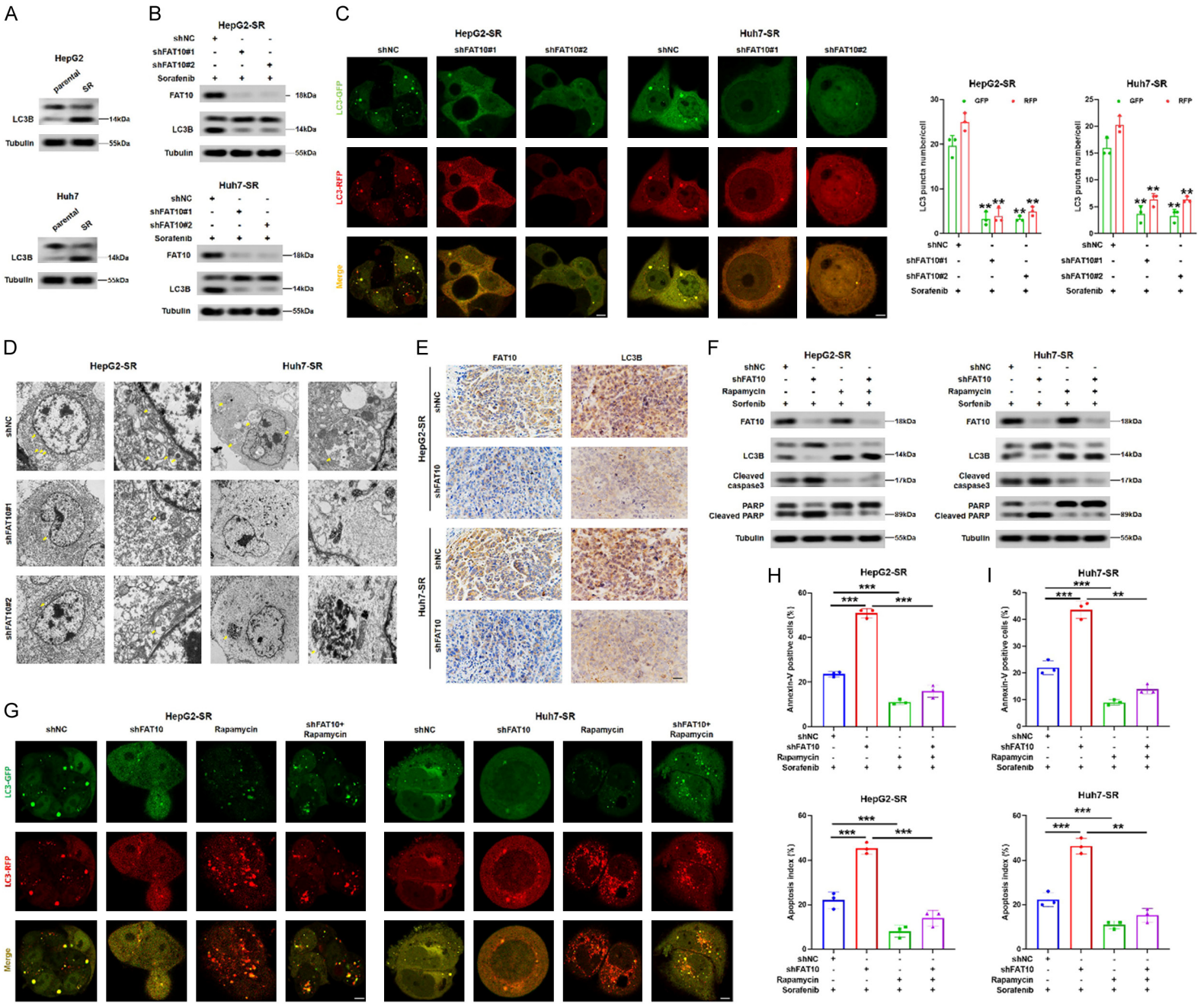
A
HepG2
parental
SR
LC3B
14kDa
Tubulin
55kDa
Huh7
B
HepG2-SR
shNC
shFAT10#1
shFAT10#2
Sorafenib
FAT10
18kDa
LC3B
14kDa
Tubulin
55kDa
Huh7-SR
C
HepG2-SR
Huh7-SR
shNC
shFAT10#1
shFAT10#2
LC3-GFP
LC3-RFP
Merge
GFP
RFP
LC3 puncta number/cell
D
HepG2-SR
Huh7-SR
shNC
shFAT10#1
shFAT10#2
E
FAT10
LC3B
HepG2-SR
Huh7-SR
shNC
shFAT10
F
HepG2-SR
Huh7-SR
shNC
shFAT10
Rapamycin
Sorfenib
FAT10
18kDa
LC3B
14kDa
Cleaved caspase3
17kDa
PARP
Cleaved PARP
89kDa
Tubulin
55kDa
G
HepG2-SR
Huh7-SR
shNC
shFAT10
Rapamycin
shFAT10+ Rapamycin
LC3-GFP
LC3-RFP
Merge
H
HepG2-SR
Annexin-V positive cells (%)
Apoptosis index (%)
shNC
shFAT10
Rapamycin
Sorafenib
I
Huh7-SR
Annexin-V positive cells (%)
Apoptosis index (%)

Figure 2. Knockdown of FAT10 expression promotes sorafenib-induced apoptosis by inhibiting autophagy in HCC-SR cells. (A) Western blot analysis of LC3B expression in parental and HepG2-SR cells and Huh7-SR cells. (B) Western blot analysis of FAT10 and LC3B expression in shNC- or shFAT10-transfected HepG2-SR cells and Huh7-SR cells after exposure to sorafenib for 24 h. (C) shNC- or shFAT10-transfected HepG2-SR cells and Huh7-SR cells were treated with sorafenib for 24 h and then transiently transfected with mRFP-GFP-LC3B plasmid for another 24 h. Scale bars: 10 μm. (D) Ultrastructural analysis of the shNC and shFAT10 groups. The yellow arrowhead represents autophagic vacuoles (defined to include autophagosomes and autolysosomes). Scale bars: 50 μm. (E) IHC detected the expression of FAT10 in subcutaneous xenografts. Scale bars: 100 μm. (F) Western blot analysis of LC3B, cleaved caspase, PARP, and cleaved PARP expression in shNC- or shFAT10-transfected HepG2-SR cells and Huh7-SR cells treated with or without rapamycin (5 μM). (G) shNC- or shFAT10-transfected HepG2-SR cells and Huh7-SR cells treated with or without rapamycin and then transiently transfected with mRFP-GFP-LC3B plasmid for 24 h. Scale bars: 10 μm. (H and I) Flow cytometry analysis (H) and TUNEL assay (I) detection of cell apoptosis in HepG2-SR cells and Huh7-SR cells with the indicated treatments. $^{**}P < 0.01$, $^{***}P < 0.001$.

NEDD4 in shNC HCC-SR cells and shFAT10 HCC-SR cells. qRT-PCR and Western blot results showed that compared with the shNC HCC-SR cells, the expression of NEDD4 mRNA in shFAT10 HCC-SR cells remained unchanged, while the expression of protein decreased (**Figure 4B**). Moreover, overexpressing NEDD4 mitigated FAT10 knockdown-induced the upregulation of PTEN expression, the inhibition of autophagy mediated by the AKT pathway and the upregulation of sorafenib-induced apoptosis in HCC-SR cells (**Figure 4C-F**). In addition, we investigated the expression of FAT10 and NEDD4 in sorafenib-resistant and sorafenib-sensitive HCC tissues. Our results revealed that FAT10 and NEDD4 were highly expressed in sorafenib-resistant tissues (Figure S4A, S4B). Overall, our data indicate that downregulating FAT10 in HCC-SR cells upregulates PTEN expression through NEDD4, and subsequently inhibits AKT-pathway-mediated autophagy, thereby enhancing sensitivity to sorafenib.

FAT10 stabilizes NEDD4 expression by antagonizing its ubiquitination in HCC cells

Next, we investigated the molecular mechanism by which FAT10 regulates NEDD4 expression. Our previous studies showed that FAT10 can stabilize the expression of substrate proteins by antagonizing its ubiquitination [17-20]. In addition, studies have confirmed that NEDD4 could be degraded by the ubiquitin proteasome pathway [37, 38]. Therefore, we speculate that FAT10 could stabilize its protein expression by antagonizing the ubiquitination of NEDD4. Our results confirm that FAT10 and NEDD4 can bind to each other in HepG2 and Huh7 cells. The LC-MS/MS results showed that NEDD4 can bind to FAT10 in HCC cells (Table S1). Docking analysis also revealed an interaction between NEDD4 and FAT10 (**Figure 5A**). Co-IP and confocal microscopy colocalization analysis showed that NEDD4 and FAT10 can combine with each other (**Figures 5B**, **5C**, S5A). Furthermore, our results show that FAT10 regulates NEDD4 protein expression by affecting its proteasome pathway degradation in HCC cells. Western blot analysis showed that reducing or increasing FAT10 expression altered the protein levels of NEDD4, whereas these effects were not evident after HCC cells were treated with MG132 (**Figures 5D**, S5B). Western blot analysis also showed that altering the expression of FAT10 can affect the stability of NEDD4 protein in HCC cells (**Figures 5E**, S5C). Finally, our data indicate that overexpressed FAT10 can compete with Ub to bind NEDD4, which leads to an increase in the FAT10-NEDD4 complex, thus inhibiting its ubiquitination level. A glutathione S-transferase (GST) pulldown assay showed that as FAT10 expression increased, the levels of the FAT10-NEDD4 complexes gradually increased, whereas the levels of the Ub-NEDD4 complexes gradually decreased (**Figures 5F**, **5G**, S5D). The Co-IP and in vivo ubiquitination assay results showed that the downregulation of FAT10 increased the ubiquitination level of NEDD4 and that FAT10 overexpression decreased the ubiquitination level of NEDD4 in HCC cells (**Figures 5H**, S5E). Taken together, our data confirm that FAT10 stabilizes protein expression by antagonizing the ubiquitination of NEDD4 in HCC cells.

FAT10-NEDD4 complexes are not degraded by proteasomes in HCC cells

Our previous studies showed that FAT10 competes with Ub to bind eukaryotic translation elongation factor 1A1 (eEF1A1) to form the FAT10-eEF1A1 complex, which is not recognized by the only FAT10 receptor, RPN10, in the

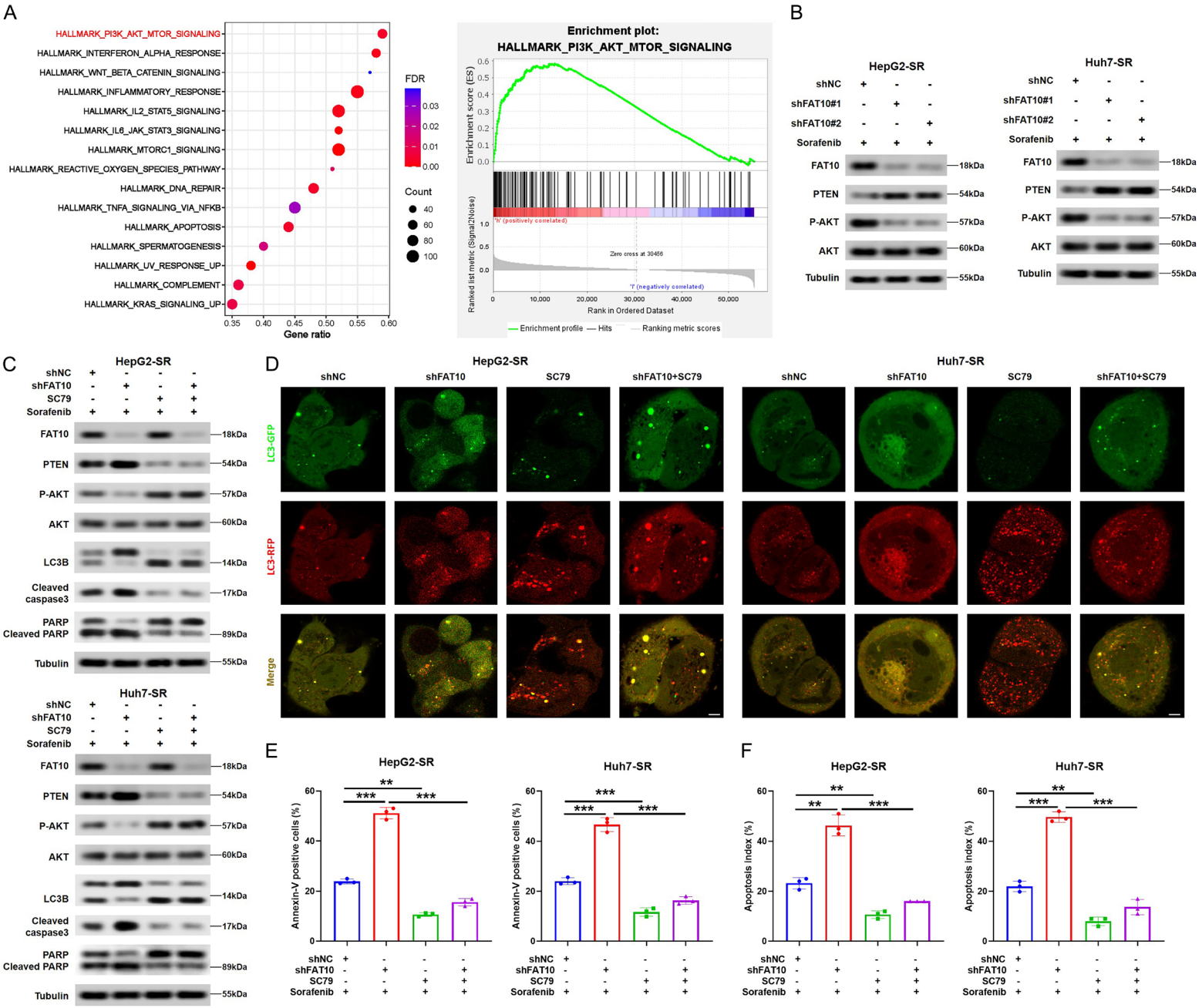
A
HALLMARK_PI3K_AKT_MTOR_SIGNALING
HALLMARK_INTERFERON_ALPHA_RESPONSE
HALLMARK_WNT_BETA_CATENIN_SIGNALING
HALLMARK_INFLAMMATORY_RESPONSE
HALLMARK_IL2_STAT5_SIGNALING
HALLMARK_IL6_JAK_STAT3_SIGNALING
HALLMARK_MTORC1_SIGNALING
HALLMARK_REACTIVE_OXYGEN_SPECIES_PATHWAY
HALLMARK_DNA_REPAIR
HALLMARK_TNFA_SIGNALING_VIA_NFKB
HALLMARK_APOPTOSIS
HALLMARK_SPERMATOGENESIS
HALLMARK_UV_RESPONSE_UP
HALLMARK_COMPLEMENT
HALLMARK_KRAS_SIGNALING_UP
0.35 0.40 0.45 0.50 0.55 0.60
Gene ratio
FDR
0.03
0.02
0.01
0.00
Count
40
60
80
100
Enrichment plot:
HALLMARK_PI3K_AKT_MTOR_SIGNALING
Enrichment score (ES)
Ranked list metric (Signal2Noise)
'h' (positively correlated)
Zero cross at 30466
't' (negatively correlated)
Rank in Ordered Dataset
Enrichment profile
Hits
Ranking metric scores
B
HepG2-SR
shNC
shFAT10#1
shFAT10#2
Sorafenib
FAT10
PTEN
P-AKT
AKT
Tubulin
18kDa
54kDa
57kDa
60kDa
55kDa
Huh7-SR
C
HepG2-SR
shNC
shFAT10
SC79
Sorafenib
FAT10
PTEN
P-AKT
AKT
LC3B
Cleaved caspase3
PARP
Cleaved PARP
Tubulin
18kDa
54kDa
57kDa
60kDa
14kDa
17kDa
89kDa
55kDa
Huh7-SR
D
HepG2-SR
Huh7-SR
shNC
shFAT10
SC79
shFAT10+SC79
LC3-GFP
LC3-RFP
Merge
E
HepG2-SR
Huh7-SR
Annexin-V positive cells (%)
F
HepG2-SR
Huh7-SR
Apoptosis index (%)

Figure 3. Downregulation of FAT10 promotes sorafenib-induced apoptosis by upregulating PTEN to inhibit AKT pathway-mediated autophagy in HCC-SR cells. (A) Gene set enrichment analysis for the enriched underlying biological pathways between high and low expression of FAT10. (B) Western blot analysis of PTEN, AKT and p-AKT expression in shNC- or shFAT10-transfected HepG2-SR cells and Huh7-SR cells after exposure to sorafenib for 24 h. (C) Western blot analysis of PTEN, AKT, p-AKT, LC3B, cleaved caspase, PARP, and cleaved PARP expression in shNC- or shFAT10-transfected HepG2-SR cells and Huh7-SR cells treated with or without sc79 (1 nM). (D) shNC- or shFAT10-transfected HepG2-SR cells and Huh7-SR cells treated with or without sc79 and then transiently transfected with mRFP-GFP-LC3B plasmid for 24 h. Scale bars: 10 μm. (E and F) Flow cytometry analysis (E) and TUNEL assay (F) detection of cell apoptosis in HepG2-SR cells and Huh7-SR cells with the indicated treatments. $^{**}P < 0.01$, $^{***}P < 0.001$.

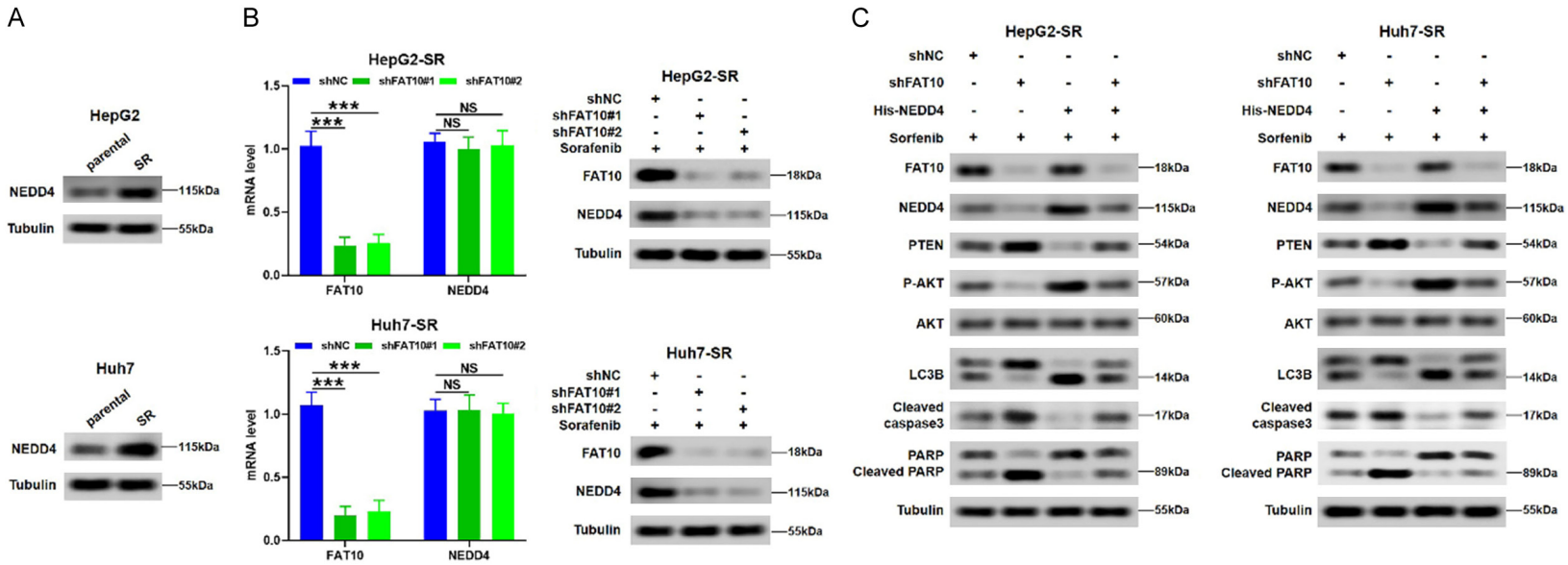

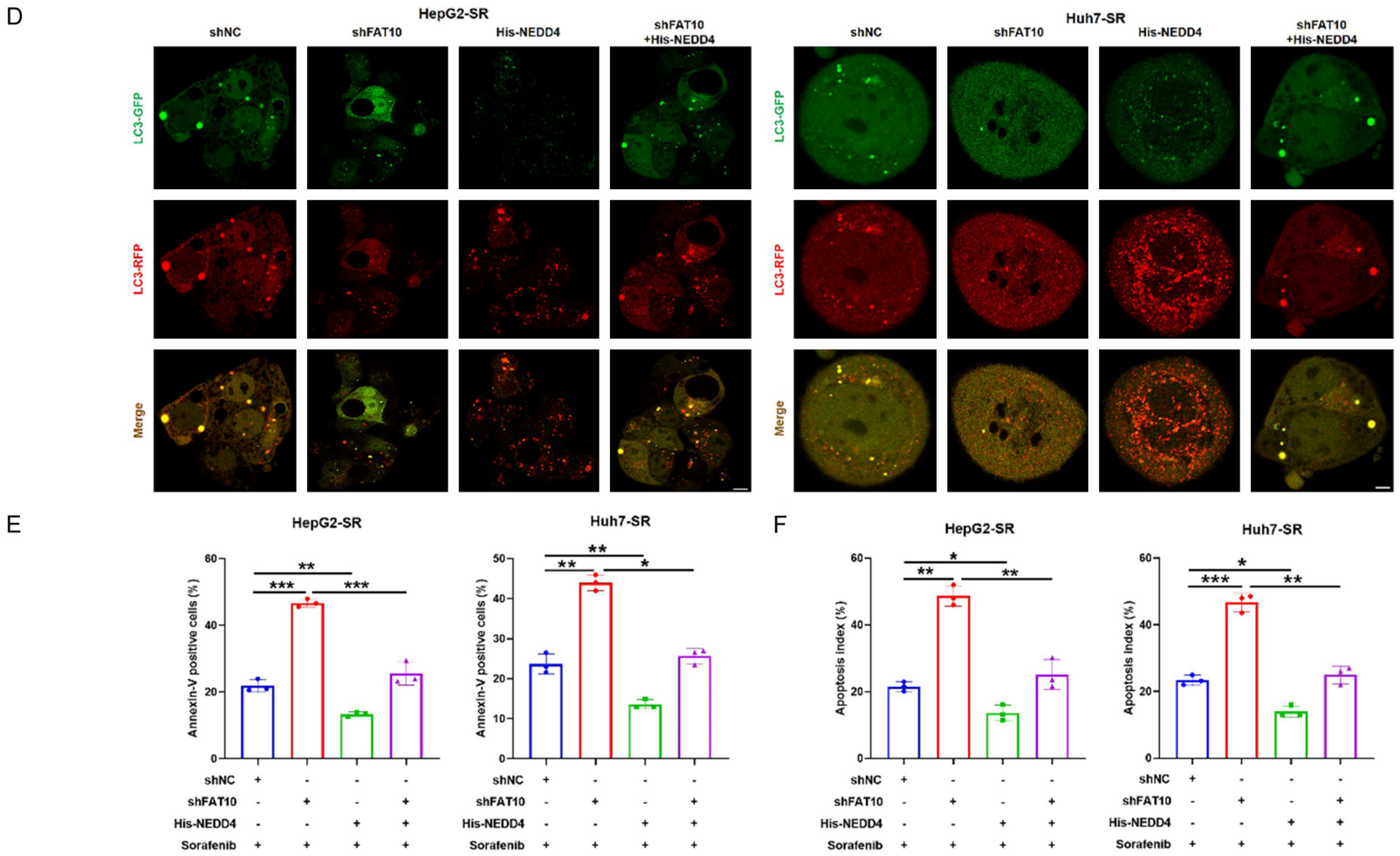

Figure 4. Downregulation of FAT10 promotes sorafenib-induced apoptosis by inhibiting the NEDD4-mediated PTEN/AKT pathway in HCC-SR cells. (A) Western blot analysis of NEDD4 expression in parental and HepG2-SR cells and Huh7-SR cells. (B) qRT-PCR analysis and Western blot analysis of NEDD4 expression in shNC- or shFAT10-transfected HepG2-SR cells and Huh7-SR cells after exposure to sorafenib for 24 h. (C) Western blot analysis of PTEN, AKT, p-AKT, LC3B, cleaved caspase, PARP, and cleaved PARP expression in shNC- or shFAT10-transfected HepG2-SR cells and Huh7-SR cells, with or without NEDD4 overexpression. (D) shNC- or shFAT10-transfected HepG2-SR cells and Huh7-SR cells, with or without NEDD4 overexpression, were then transiently transfected with mRFP-GFP-LC3B plasmid for 24 h. Scale bars: 10 μm. (E and F) Flow cytometry analysis (E) and TUNEL assay (F) detection of cell apoptosis in HepG2-SR cells and Huh7-SR cells with the indicated treatments. *$P < 0.05$, **$P < 0.01$, ***$P < 0.001$, NS, not significant.

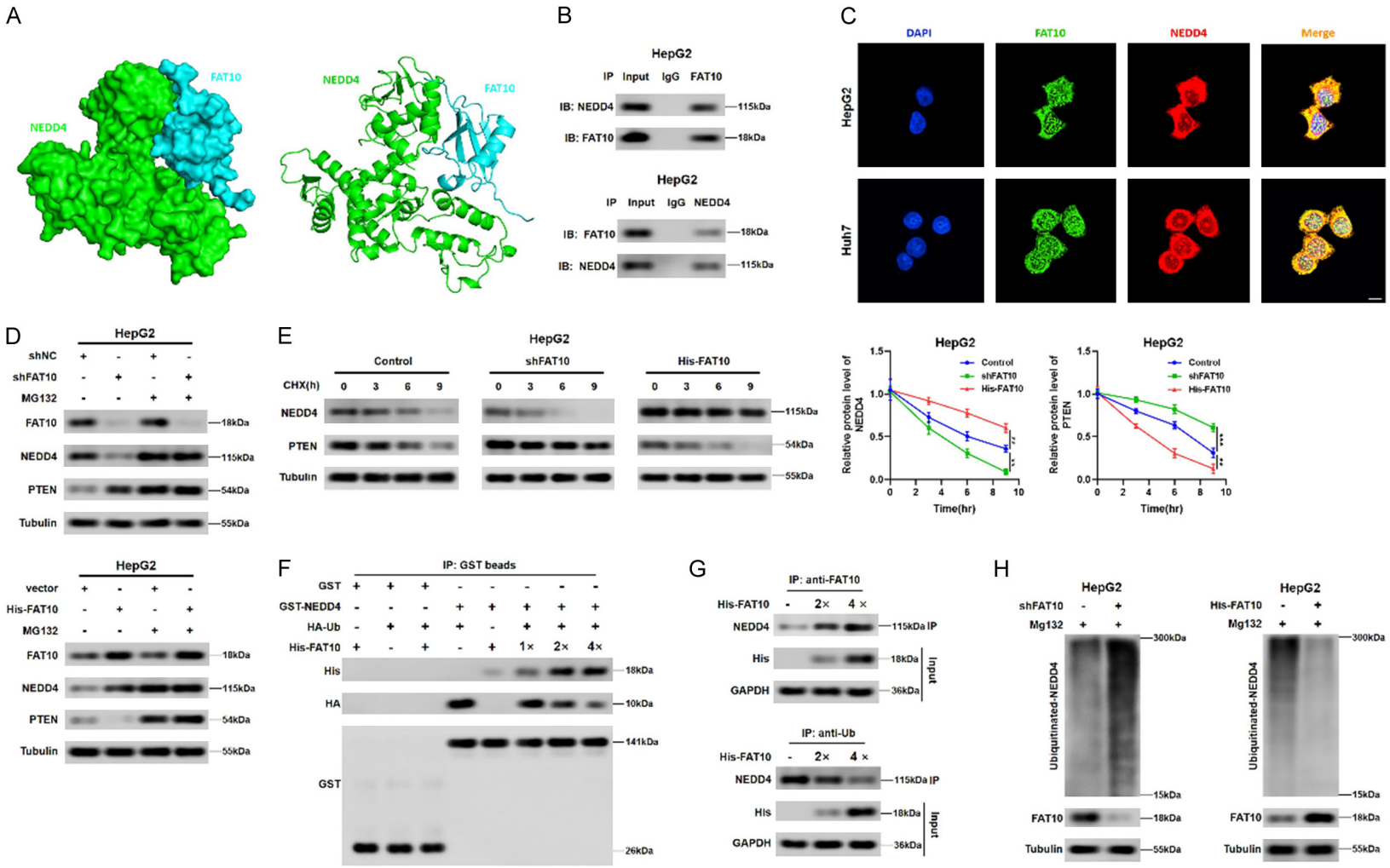

Figure 5. FAT10 stabilizes NEDD4 expression by antagonizing its ubiquitination in HCC cells. A. Docking analysis for the binding of FAT10 and NEDD4. B. Co-IP for FAT10 and NEDD4 in HepG2 cells. C. Colocalization of FAT10 and NEDD4 in HepG2 and Huh7 cells. D. Western blot analysis of NEDD4 and PTEN expression in shNC- or shFAT10-transfected HepG2 cells treated with or without MG132 (15 μM). E. The cells were subjected to CHX (20 μmol/l) exposure at the indicated times, and the degradation of exogenous NEDD4 and PTEN was detected in HepG2 cells transfected with the indicated plasmids. F. Binding of NEDD4 during the course of the competition was analyzed by GST pulldown experiments. G. Huh7 cells were transfected with increasing amounts of Flag-FAT10 plasmid. The cells were lysed for immunoprecipitation using anti-Ub and anti-FAT10 beads to detect NEDD4 binding. H. HepG2 cells were transfected with the indicated plasmid. The cells in each group were treated with MG132. The ubiquitination of NEDD4 was detected.

26S proteasome and is not degraded by proteasomes, resulting in increased expression of the eEF1A1 protein in 293 cells [17]. Therefore, we aimed to further investigate whether the FAT10-NEDD4 complex is also not recognized by RPN10 and thus not degraded by the proteasome in HCC cells. To do this, we first constructed the HA-FAT10-p62 fusion plasmid as a positive control to observe whether the FAT10-NEDD4 complex was degraded by the proteasome in HCC cells. In addition, to eliminate the effect of endogenous FAT10 on the expression of substrate proteins, we generated FAT10 knockout (HepG2 FAT10$^{-/-}$ and Huh7 FAT10$^{-/-}$) HCC cell lines. Interestingly, our results confirm that the FAT10-NEDD4 complex is not recognized by RPN10 and likewise not degraded by proteasomes in HCC cells. This conclusion was based on the following observations. First, HA-FAT10-p62 is degrade by the proteasome in HCC cells, whereas HA-FAT10-NEDD4 is not. Western blot analysis showed that HA-FAT10-p62 expression significantly increased with MG132 treatment in FAT10$^{-/-}$ HCC cells, while the expression of HA-FAT10-NEDD4 remained unchanged irrespective of MG132 treatment (**Figure 6A**). Second, altering the expression of RPN10 do not affect the proteasomal degradation of the FAT10-NEDD4 complex in FAT10$^{-/-}$ HCC cells. Western blot analysis showed that reducing or increasing RPN10 expression altered the half-life of ectopically expressed HA-FAT10-p62; however, reducing or increasing the expression of RPN10 had no effect on the degradation rate of HA-FAT10-NEDD4 in FAT10$^{-/-}$ HCC cells (**Figure 6B**). Third, to exclude the effect of Ub on the degradation of the FAT10-NEDD4 complex, we generated HCC cell lines with stable low expression of Ub (shUb HepG2/shUb Huh7). Our results show that RPN10 cannot recognize the FAT10-NEDD4 complex in HCC cells, which means that the FAT10-NEDD4 complex is not degraded by proteasomes. The Co-IP and Western blot analysis results showed that the expression of the FAT10-P62 complex, FAT10-NEDD4 complex, P62 and NEDD4 was altered with changes in RPN10 in shNC HCC cells; however, in shUb HCC cells, changing the expression of RPN10 also altered the expression of the FAT10-P62 complex and P62 but not the expression of the FAT10-NEDD4 complex and NEDD4 (**Figure 6C**).

Targeting FAT10 inhibits the NEDD4-PTEN/AKT axis to enhance sorafenib sensitivity in HCC-SR cells

Our results confirm that the expression of FAT10 in HCC-SR cells increases, which can induce HCC cell sorafenib resistance by promoting NEDD4-PTEN/AKT axis-mediated autophagy. Thus, we aimed to find a drug that targets FAT10 to inhibit NEDD4-PTEN/AKT axis-mediated autophagy, thereby increasing the sensitivity of HCC-SR cells to sorafenib. We screened the small molecule Compound 7695-0983, which inhibits the expression of FAT10, through the ChemDiv database. Protein structure and drug target analysis indicated that the small molecule Compound 7695-0983 (PubChem CID 328269049, Ethyl 4-(3-hydroxyphenyl)-2-methyl-1,4-dihydropyrimido [1,2-a] benzimidazole-3-carboxylate) binds to the active pocket of FAT10 (**Figure 7A-D**). Next, we investigated whether the small molecule Compound 7695-0983 can enhance the sensitivity of HCC-SR cells to sorafenib. First, our in vitro results show that treatment with the small molecule Compound 7695-0983 combined with sorafenib could inhibit FAT10 to inhibit NEDD4-PTEN/AKT axis-mediated autophagy to increase sorafenib-induced apoptosis. Western blot analysis showed that compared with the sorafenib treatment group alone, the expression of FAT10, NEDD4, p-AKT and autophagy-related proteins decreased, and the expression of PTEN and apoptosis-related proteins increased in the combined treatment group (**Figures 7E**, S6A). The flow cytometric and TUNEL results showed that the combined treatment group of HCC-SR cells exhibited a higher apoptosis rate than the single treatment group of sorafenib (**Figures 7F**, **7G**, S6B, S6C). Our in vivo data also confirm that small molecules combined with sorafenib treatment can inhibit FAT10 and then inhibit NEDD4-PTEN/AKT axis-mediated autophagy to increase the sensitivity to sorafenib. We constructed a nude mouse subcutaneous tumor-bearing model using HCC-SR cells and investigated the therapeutic effects of sorafenib alone or in combination with the small molecule Compound 7695-0983. The results showed that compared with the sorafenib alone treatment group, the combined treatment group tumor volume was significantly decreased, with a significantly reduced tumor weight and a slower

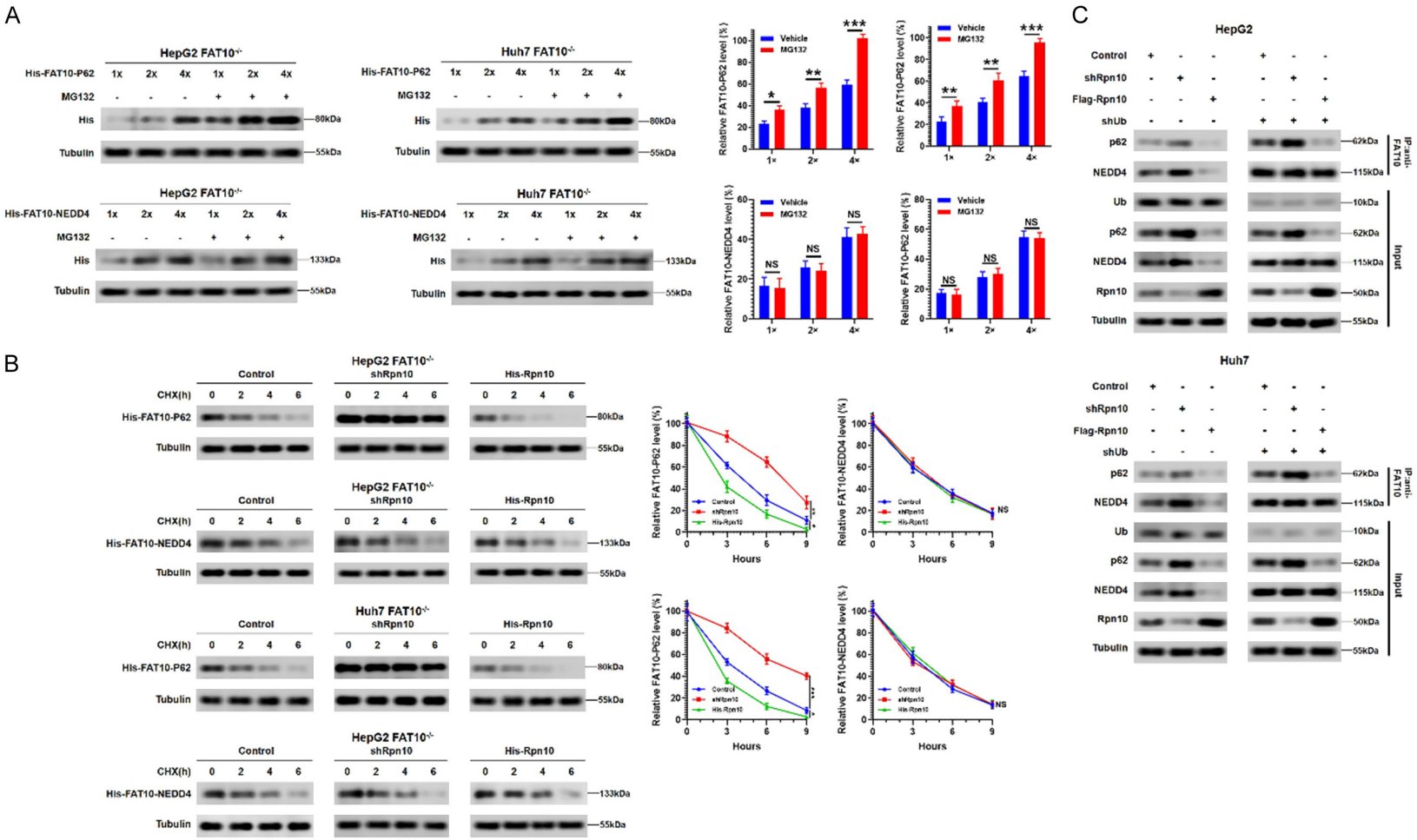

Figure 6. FAT10-NEDD4 complexes are not degraded by proteasomes in HCC cells. A. HA-FAT10-p62 and HA-FAT10-NEDD4 fusion plasmids were transfected into FAT10$^{-/-}$ HepG2 and FAT10$^{-/-}$ Huh7 cells at different doses. The expression of HA-FAT10-p62 and HA-FAT10-NEDD4 complexes was observed with or without MG132 (10 μg/ml). B. shUb FAT10$^{-/-}$ HepG2 and shUb FAT10$^{-/-}$ Huh7 cells were transfected with HA-FAT10-p62 and HA-FAT10-NEDD4 plasmids combined with His-Rpn10 or shRpn10 plasmids and were then subjected to cycloheximide (CHX, 20 μg/mL) exposure. Western blot analysis was performed for the indicated proteins and quantified by ImageJ software. C. shUb/shNC-HepG2 and shUb/shNC-Huh7 cells were transfected with His-Rpn10 or shRpn10, respectively. The cell lysates were subjected to Co-IP and Western blot analyses for FAT10-p62, p62, FAT10-NEDD4, and NEDD4. *P < 0.05, **P < 0.01, ***P < 0.001.

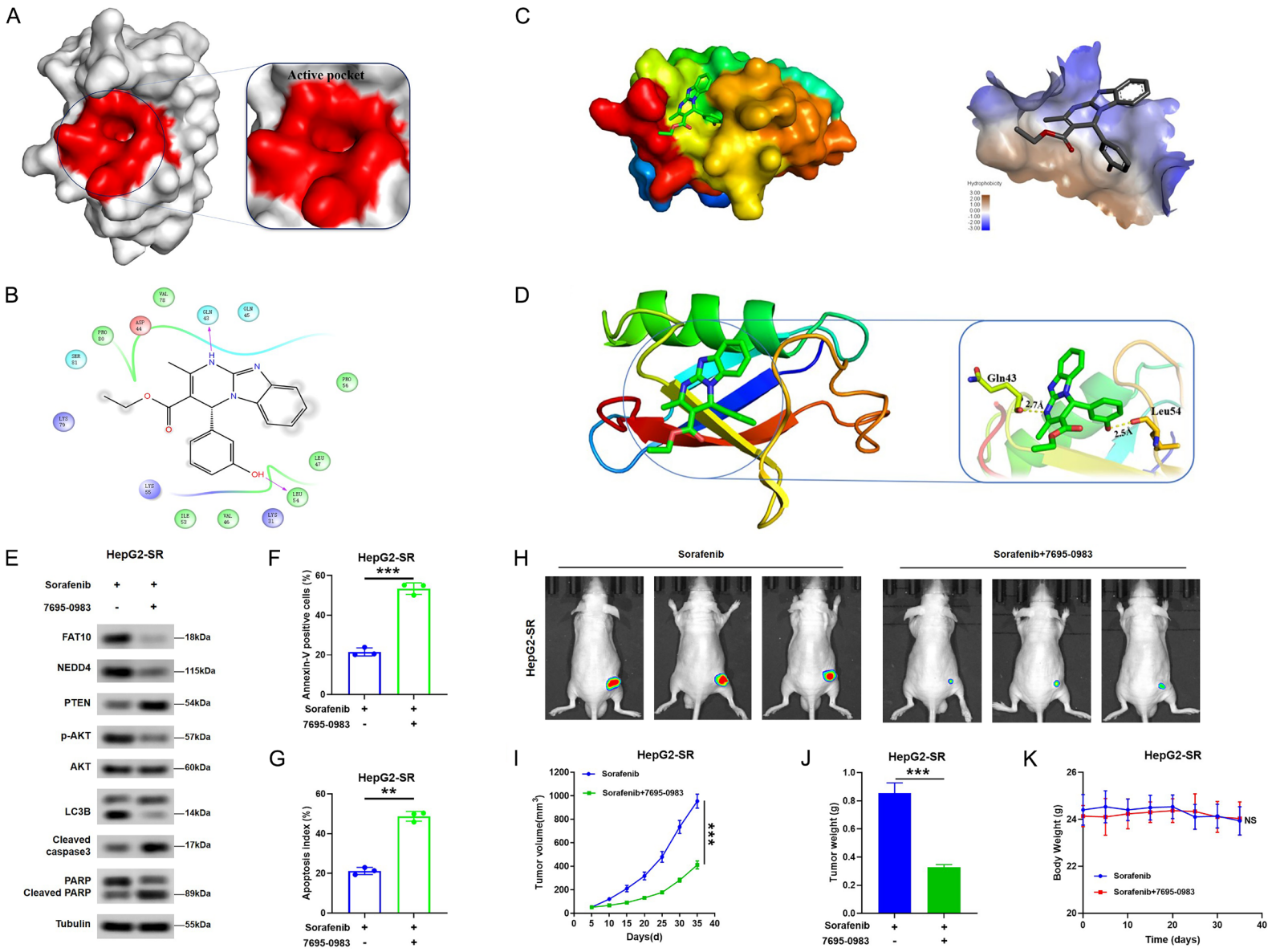
A
Active pocket
B
C
D
Gln43
Leu54
2.7Å
2.5Å
E
HepG2-SR
Sorafenib + +
7695-0983 - +
FAT10 18kDa
NEDD4 115kDa
PTEN 54kDa
p-AKT 57kDa
AKT 60kDa
LC3B 14kDa
Cleaved caspase3 17kDa
PARP Cleaved PARP 89kDa
Tubulin 55kDa
F
HepG2-SR
***
Annexin-V positive cells (%)
Sorafenib + +
7695-0983 - +
G
HepG2-SR
**
Apoptosis index (%)
Sorafenib + +
7695-0983 - +
H
Sorafenib
Sorafenib+7695-0983
HepG2-SR
I
HepG2-SR
Sorafenib
Sorafenib+7695-0983
Tumor volume(mm3)
***
Days(d)
J
HepG2-SR
***
Tumor weight (g)
Sorafenib + +
7695-0983 - +
K
HepG2-SR
NS
Body Weight (g)
Sorafenib
Sorafenib+7695-0983
Time (days)

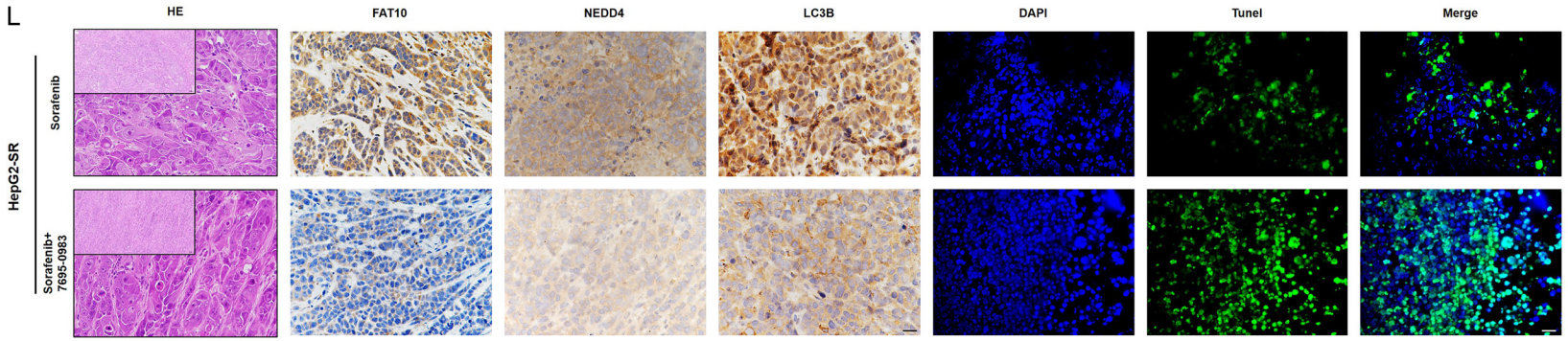

Figure 7. Targeting FAT10 inhibits the NEDD4-PTEN/AKT axis to enhance sorafenib sensitivity in HCC-SR cells. (A) FAT10 active pocket. (B) Chemical structure of small molecule Compound 7695-0983. (C and D) Protein structure and drug target analyses revealed that the small-molecule Compound 7695-0983 binds to the active pocket of FAT10. (E) Western blot analysis of NEDD4, PTEN, AKT, p-AKT, LC3B, cleaved caspase, PARP, and cleaved PARP in HepG2-SR cells treated with sorafenib alone or combined with 7695-0983. (F and G) Flow cytometry analysis (F) and TUNEL assay (G) detection of cell apoptosis in HepG2-SR cells treated with sorafenib alone or combined with 7695-0983. (H) Nude mice injected with luciferase-expressing HepG2-SR cells were treated with sorafenib alone or combined with 7695-0983 intraperitoneally, and then subcutaneous xenografts were assessed by an IVIS imaging system (n = 3). (I and J) The (I) weights and (J) volumes of subcutaneous tumors were measured. (K) Nude mouse body weights were recorded. (L) IHC detected the expression of FAT10, NEDD4, and LC3B in subcutaneous xenografts and representative figures of TUNEL staining showing apoptotic cells (stained in green) in subcutaneous xenografts. Scale bars: 100 μm. $^{**}P < 0.01$, $^{***}P < 0.001$.

growth rate (**Figures 7H-J**, S6D-F). In addition, compared with the sorafenib alone treatment group, no significant changes in the body weight of mice were observed in the combined treatment group of Compound 7695-0983 and sorafenib (**Figures 7K**, S6G). IHC analysis further showed that the expression of FAT10 and NEDD4 and autophagy levels in tumor tissues in the combined treatment group were lower than those in the sorafenib alone treatment group, and the TUNEL results showed that HCC cell apoptosis in tumor tissue in the combination treatment group of small molecule Compound 7695-0983 and sorafenib was significantly increased (**Figures 7L**, S6H). Thus, our data demonstrate that the small molecule Compound 7695-0983 can inhibit the expression of FAT10 to inhibit NEDD4-PTEN/AKT axis-mediated autophagy, thereby increasing the sensitivity of HCC-SR cells to sorafenib in vivo and in vitro.

Discussion

HCC is the fifth most common cancer in the world, with an increasing incidence worldwide, and it is the fourth leading cause of cancer-related death globally [39]. Due to the difficulty of early diagnosis, most patients with HCC are already in advanced stages at the time of diagnosis, losing the opportunity to undergo surgery or ablation treatment [40]. Therefore, the development of drugs for patients with advanced HCC is of great value in prolonging their survival and improving their quality of life. Sorafenib is the first standard first-line systemic treatment drug approved by the FDA for patients with advanced HCC [41]. Sorafenib is a multitarget tyrosine kinase inhibitor that inhibits tumor growth and angiogenesis by inhibiting intracellular Raf kinase and cell surface kinase receptors in the treatment of tumors [42]. In clinical trials, sorafenib has been proven to prolong the survival of patients with advanced HCC by approximately three months, setting the gold standard for frontline systemic drug therapy in the treatment of advanced HCC [43, 44]. However, with the extensive use of sorafenib in clinical practice, only 30% of patients can benefit from sorafenib therapy, and this population usually develops drug resistance within six months, increasing the risk of cancer recurrence and presenting significant challenges to the treatment of HCC patients with sorafenib [45]. Although researchers have carried out structural modifications based on sorafenib and upgraded iterative TKI-targeted drugs, such as lenvatinib, regorafenib and donafenib, the clinical treatment efficacy is still poor because of the progressive development of drug resistance in patients [46]. Therefore, further identification of key factors involved in mediating the sorafenib-resistance of HCC cells and exploration of the underlying mechanisms are of great value for the future development of novel TKI-targeted drugs based on sorafenib. In this study, we observed the high expression of FAT10 in sorafenib-resistant HCC cells by generating sorafenib-resistant HCC cell lines and knocking down the expression of FAT10 in sorafenib-resistant HCC cells enhance their sensitivity to sorafenib in vitro and in vivo. Further studies have shown that knockdown of FAT10 expression in sorafenib-resistant HCC cells can significantly suppress the level of autophagy in sorafenib-resistant HCC cells and that treatment with the autophagy activator rapamycin can reverse the reduction in cell autophagy levels caused by knockdown of FAT10 and increase the sensitivity of sorafenib-resistant HCC cells to sorafenib. Next, we found that reducing the expression of FAT10 in sorafenib-resistant HCC cells can significantly promote the expression of PTEN and inhibit the AKT signaling pathway in sorafenib-resistant HCC cells. Furthermore, we found that treatment with the specific AKT signaling activator SC79 can also reverse the reduction in cell autophagy and increased sensitivity of resistant cells to sorafenib caused by FAT10 knockdown. These findings indicate that FAT10 is a key factor involved in mediating sorafenib-resistant of HCC cells by downregulating PTEN expression to induce AKT-mediated autophagy.

E3 ligases can be divided into three main types based on the presence of characteristic domains and the mechanism of ubiquitin transfer to substrate proteins: the truly interesting new gene (RING) finger family, the HECT family, and the RING between RING (RBR) family [47]. NEDD4, a HECT-type E3 ubiquitin ligase, has attracted much attention in regard to tumors. Studies have found that NEDD4 is highly expressed in various tumor tissues and is closely related to the pathological characteris-

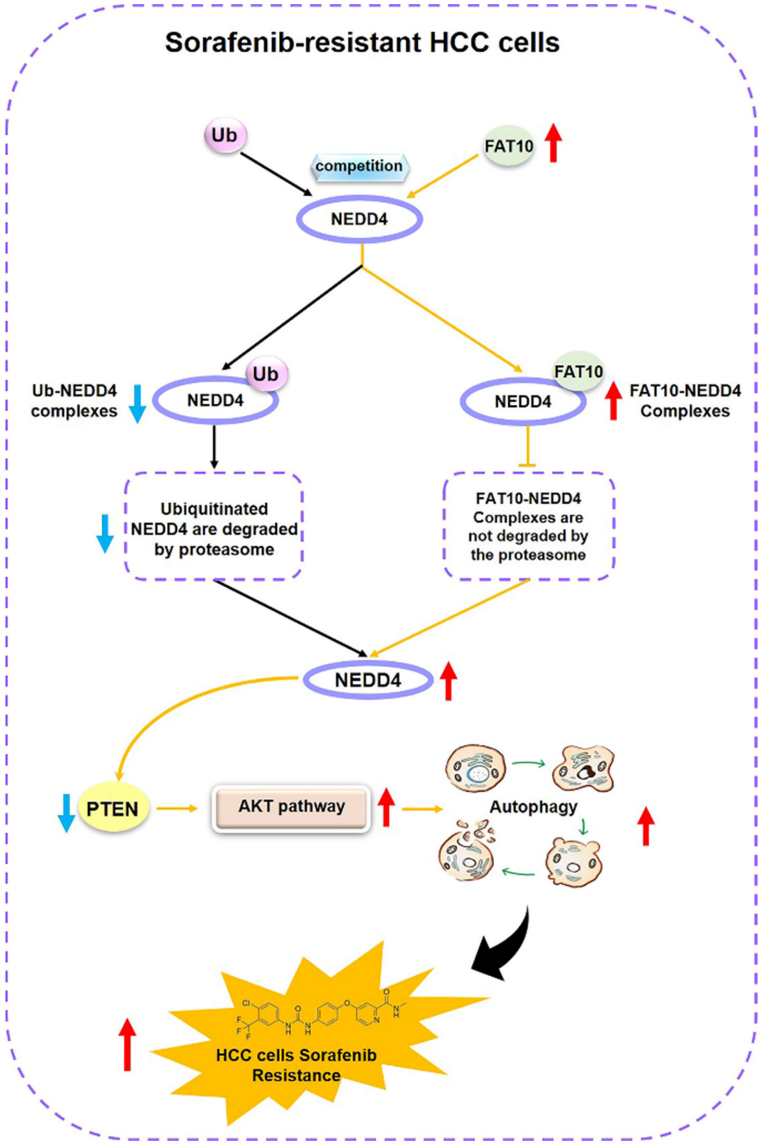

Figure 8. The mechanism by which FAT10 promotes sorafenib resistance in HCC cells. The expression of FAT10 increased in HCC-SR cells, which stabilized the protein expression of the PTEN-specific E3 ubiquitin ligase NEDD4, increased autophagy mediated by the PTEN/AKT signaling pathway, and promoted sorafenib resistance in HCC cells.

tics and poor prognosis of tumor patients [48]. Knockdown of NEDD4 expression can significantly inhibit the malignant phenotype of tumor cells [49]. The mechanisms of regulating the expression of NEDD4 to affect the occurrence and development of cancers are complex [48]. Our results confirm that FAT10 can stabilize the protein expression of NEDD4 and then downregulate PTEN expression, thereby inducing AKT-mediated autophagy to promote the resistance of HCC cells to sorafenib. This conclusion is based on the following observations. First, the expression of NEDD4 was increased in sorafenib-resistant HCC cells, and reducing the expression of FAT10 in sorafenib-resistant HCC cells reduced the protein expression of NEDD4 but did not affect its mRNA expression level. Second, knocking down the expression of FAT10 in sorafenib-resistant HCC cells reduced the expression levels of NEDD4, which caused downregulation of PTEN, thereby inducing AKT-mediated autophagy and promoting the sensitivity of sorafenib-resistant HCC cells to sorafenib. Third, on the one hand, FAT10 can antagonize the ubiquitination of NEDD4, inhibiting its degradation; on the other hand, the FAT10-NEDD4 complex is not degraded by the proteasome, and these effects lead to the stabilization of NEDD4 protein expression by FAT10. Finally, we screened the small molecule Compound 7695-0983 through protein structure and drug target analysis, and the results show that it can inhibit the expression of FAT10 to inhibit NEDD4-PTEN/AKT axis-mediated autophagy, thereby increasing the sensitivity of sorafenib-resistant HCC cells to sorafenib. Therefore, combined with our results in vivo and in vitro, we established a mechanistic model to describe how FAT10 mediates sorafenib resistance in HCC cells (**Figure 8**). The expression of FAT10 was increased in sorafenib-resistant HCC cells. On the one hand, FAT10 inhibits NEDD4 ubiquitination through reduced Ub-NEDD4 complexes. On the other hand, the expression of NEDD4 increases with the increase of FAT10-NEDD4 complexes, which are not degraded by proteasomes. These effects lead to FAT10 stabilizing NEDD4 protein

expression, which cause downregulation of PTEN, thereby inducing AKT-mediated autophagy, and ultimately promoting sorafenib resistance in HCC cells. To the best of our knowledge, this is the first study to identify FAT10 as a key factor in sorafenib resistance in HCC cells and explain its underlying mechanism in the preclinical model.

Conclusion

By constructing sorafenib-resistant HCC cell lines, our preclinical study found that FAT10 stabilizes the protein expression of PTEN-specific E3 ubiquitin ligase NEDD4, which in turn enhances PTEN/AKT pathway-induced autophagy to mediate sorafenib-resistant of HCC cells. In the future, further exploration is warranted regarding the relationship between the expression of FAT10 in HCC tissues and the sensitivity of patients with HCC to sorafenib, in addition to determining why FAT10 is highly expressed in sorafenib-resistant HCC cells. These studies will provide new strategies for the development of new TKI targeted drugs based on sorafenib for the treatment of advanced HCC in the future.

Acknowledgements

This work was supported by National Natural Science Foundation of China (82160486, 81773126 and 81560475), the National Key R&D Program of China (2016YFC0900400), and the Project of Jiangxi Provincial Department of Science and Technology (20223BCG-74008 and 20212ACB206024).

Disclosure of conflict of interest

None.

Address correspondence to: Jianghua Shao and Leifeng Chen, Department of General Surgery, The Second Affiliated Hospital of Nanchang University, Nanchang 330000, Jiangxi, China. E-mail: shao5022@163.com (JHS); 18770099029@126.com (LFC)

References

[1] Parzych KR and Klionsky DJ. An overview of autophagy: morphology, mechanism, and regulation. Antioxid Redox Signal 2014; 20: 460-473.
[2] Levine B and Kroemer G. Biological functions of autophagy genes: a disease perspective. Cell 2019; 176: 11-42.
[3] Levy JMM, Towers CG and Thorburn A. Targeting autophagy in cancer. Nat Rev Cancer 2017; 17: 528-542.
[4] White E, Lattime EC and Guo JY. Autophagy regulates stress responses, metabolism, and anticancer immunity. Trends Cancer 2021; 7: 778-789.
[5] Chen N and Debnath J. Autophagy and tumorigenesis. FEBS Lett 2010; 584: 1427-1435.
[6] Chang H and Zou Z. Targeting autophagy to overcome drug resistance: further developments. J Hematol Oncol 2020; 13: 159.
[7] Qin Y, Ashrafizadeh M, Mongiardini V, Grimaldi B, Crea F, Rietdorf K, Gyorffy B, Klionsky DJ, Ren J, Zhang W and Zhang X. Autophagy and cancer drug resistance in dialogue: pre-clinical and clinical evidence. Cancer Lett 2023; 570: 216307.
[8] Zamame Ramirez JA, Romagnoli GG and Kaneno R. Inhibiting autophagy to prevent drug resistance and improve anti-tumor therapy. Life Sci 2021; 265: 118745.
[9] Heqing Y, Bin L, Xuemei Y and Linfa L. The role and mechanism of autophagy in sorafenib targeted cancer therapy. Crit Rev Oncol Hematol 2016; 100: 137-140.
[10] Prieto-Dominguez N, Ordonez R, Fernandez A, Garcia-Palomo A, Muntane J, Gonzalez-Gallego J and Mauriz JL. Modulation of autophagy by sorafenib: effects on treatment response. Front Pharmacol 2016; 7: 151.
[11] Tao H, Zhang Y, Li J, Liu J, Yuan T, Wang W, Liang H, Zhang E and Huang Z. Oncogenic lncRNA BBOX1-AS1 promotes PHF8-mediated autophagy and elicits sorafenib resistance in hepatocellular carcinoma. Mol Ther Oncolytics 2022; 28: 88-103.
[12] Wang D and Yang J. MiR-375 attenuates sorafenib resistance of hepatocellular carcinoma cells by inhibiting cell autophagy. Acta Biochim Pol 2023; 70: 239-246.
[13] Lu S, Yao Y, Xu G, Zhou C, Zhang Y, Sun J, Jiang R, Shao Q and Chen Y. CD24 regulates sorafenib resistance via activating autophagy in hepatocellular carcinoma. Cell Death Dis 2018; 9: 646.
[14] Schmidtke G, Aichem A and Groettrup M. FAT10ylation as a signal for proteasomal degradation. Biochim Biophys Acta 2014; 1843: 97-102.
[15] Cappadocia L and Lima CD. Ubiquitin-like protein conjugation: structures, chemistry, and mechanism. Chem Rev 2018; 118: 889-918.
[16] Aichem A and Groettrup M. The ubiquitin-like modifier FAT10 in cancer development. Int J Biochem Cell Biol 2016; 79: 451-461.
[17] Liu X, Chen L, Ge J, Yan C, Huang Z, Hu J, Wen C, Li M, Huang D, Qiu Y, Hao H, Yuan R, Lei J, Yu X and Shao J. The ubiquitin-like protein FAT10 stabilizes eEF1A1 expression to promote tu-

mor proliferation in a complex manner. Cancer Res 2016; 76: 4897-4907.
[18] Yuan R, Wang K, Hu J, Yan C, Li M, Yu X, Liu X, Lei J, Guo W, Wu L, Hong K and Shao J. Ubiquitin-like protein FAT10 promotes the invasion and metastasis of hepatocellular carcinoma by modifying beta-catenin degradation. Cancer Res 2014; 74: 5287-5300.
[19] Dong D, Jiang W, Lei J, Chen L, Liu X, Ge J, Che B, Xi X and Shao J. Ubiquitin-like protein FAT10 promotes bladder cancer progression by stabilizing survivin. Oncotarget 2016; 7: 81463-81473.
[20] Zhou Q, Peng X, Liu X, Chen L, Xiong Q, Shen Y, Xie J, Xu Z, Huang L, Hu J, Wan R and Hong K. FAT10 attenuates hypoxia-induced cardiomyocyte apoptosis by stabilizing caveolin-3. J Mol Cell Cardiol 2018; 116: 115-124.
[21] Yan J, Lei J, Chen L, Deng H, Dong D, Jin T, Liu X, Yuan R, Qiu Y, Ge J, Peng X and Shao J. Human leukocyte antigen F locus adjacent transcript 10 overexpression disturbs WISP1 protein and mRNA expression to promote hepatocellular carcinoma progression. Hepatology 2018; 68: 2268-2284.
[22] Qiu Y, Che B, Zhang W, Ge J, Du D, Li J, Peng X and Shao J. The ubiquitin-like protein FAT10 in hepatocellular carcinoma cells limits the efficacy of anti-VEGF therapy by accelerating VEGF-independent angiogenesis. J Adv Res 2023; [Epub ahead of print]
[23] Ingham RJ, Gish G and Pawson T. The Nedd4 family of E3 ubiquitin ligases: functional diversity within a common modular architecture. Oncogene 2004; 23: 1972-1984.
[24] Cao L, Li H, Liu X, Wang Y, Zheng B, Xing C, Zhang N and Liu J. Expression and regulatory network of E3 ubiquitin ligase NEDD4 family in cancers. BMC Cancer 2023; 23: 526.
[25] Huang X, Chen J, Cao W, Yang L, Chen Q, He J, Yi Q, Huang H, Zhang E and Cai Z. The many substrates and functions of NEDD4-1. Cell Death Dis 2019; 10: 904.
[26] Yue M, Yun Z, Li S, Yan G and Kang Z. NEDD4 triggers FOXA1 ubiquitination and promotes colon cancer progression under microRNA-340-5p suppression and ATF1 upregulation. RNA Biol 2021; 18: 1981-1995.
[27] Mao M, Yang L, Hu J, Liu B, Zhang X, Liu Y, Wang P and Li H. Oncogenic E3 ubiquitin ligase NEDD4 binds to KLF8 and regulates the microRNA-132/NRF2 axis in bladder cancer. Exp Mol Med 2022; 54: 47-60.
[28] Luo M, Li J, Yang Q, Xu S, Zhang K, Chen J, Zhang S, Zheng S and Zhou J. N4BP3 promotes breast cancer metastasis via NEDD4-mediated E-cadherin ubiquitination and degradation. Cancer Lett 2022; 550: 215926.
[29] Wang X, Trotman LC, Koppie T, Alimonti A, Chen Z, Gao Z, Wang J, Erdjument-Bromage H, Tempst P, Cordon-Cardo C, Pandolfi PP and Jiang X. NEDD4-1 is a proto-oncogenic ubiquitin ligase for PTEN. Cell 2007; 128: 129-139.
[30] Fouladkou F, Landry T, Kawabe H, Neeb A, Lu C, Brose N, Stambolic V and Rotin D. The ubiquitin ligase Nedd4-1 is dispensable for the regulation of PTEN stability and localization. Proc Natl Acad Sci U S A 2008; 105: 8585-8590.
[31] He C, Dong X, Zhai B, Jiang X, Dong D, Li B, Jiang H, Xu S and Sun X. MiR-21 mediates sorafenib resistance of hepatocellular carcinoma cells by inhibiting autophagy via the PTEN/Akt pathway. Oncotarget 2015; 6: 28867-28881.
[32] Chen L, Xu Z, Li Q, Feng Q, Zheng C, Du Y, Yuan R and Peng X. USP28 facilitates pancreatic cancer progression through activation of Wnt/beta-catenin pathway via stabilising FOXM1. Cell Death Dis 2021; 12: 887.
[33] Xu WP, Liu JP, Feng JF, Zhu CP, Yang Y, Zhou WP, Ding J, Huang CK, Cui YL, Ding CH, Zhang X, Lu B and Xie WF. miR-541 potentiates the response of human hepatocellular carcinoma to sorafenib treatment by inhibiting autophagy. Gut 2020; 69: 1309-1321.
[34] Yi H, Ye T, Ge M, Yang M, Zhang L, Jin S, Ye X, Long B and Li L. Inhibition of autophagy enhances the targeted therapeutic effect of sorafenib in thyroid cancer. Oncol Rep 2018; 39: 711-720.
[35] Liu W, Xu L, Wang X, Zhang D, Sun G, Wang M, Wang M, Han Y, Chai R and Wang H. PRDX1 activates autophagy via the PTEN-AKT signaling pathway to protect against cisplatin-induced spiral ganglion neuron damage. Autophagy 2021; 17: 4159-4181.
[36] Xu W, Zhang M, Li Y, Wang Y, Wang K, Chen Q, Zhang R, Song W, Huang Q, Zhao W and Wu J. YAP manipulates proliferation via PTEN/AKT/mTOR-mediated autophagy in lung adenocarcinomas. Cancer Cell Int 2021; 21: 30.
[37] Park JH, Kim SY, Cho HJ, Lee SY and Baek KH. YOD1 deubiquitinates NEDD4 involved in the hippo signaling pathway. Cell Physiol Biochem 2020; 54: 1-14.
[38] Liu J, Wan L, Liu P, Inuzuka H, Liu J, Wang Z and Wei W. SCF(beta-TRCP)-mediated degradation of NEDD4 inhibits tumorigenesis through modulating the PTEN/Akt signaling pathway. Oncotarget 2014; 5: 1026-1037.
[39] Siegel RL, Miller KD, Fuchs HE and Jemal A. Cancer statistics, 2022. CA Cancer J Clin 2022; 72: 7-33.
[40] Villanueva A. Hepatocellular carcinoma. N Engl J Med 2019; 380: 1450-1462.

[41] Llovet JM, Ricci S, Mazzaferro V, Hilgard P, Gane E, Blanc JF, de Oliveira AC, Santoro A, Raoul JL, Forner A, Schwartz M, Porta C, Zeuzem S, Bolondi L, Greten TF, Galle PR, Seitz JF, Borbath I, Haussinger D, Giannaris T, Shan M, Moscovici M, Voliotis D and Bruix J; SHARP Investigators Study Group. Sorafenib in advanced hepatocellular carcinoma. N Engl J Med 2008; 359: 378-390.

[42] Wilhelm SM, Carter C, Tang L, Wilkie D, McNabola A, Rong H, Chen C, Zhang X, Vincent P, McHugh M, Cao Y, Shujath J, Gawlak S, Eveleigh D, Rowley B, Liu L, Adnane L, Lynch M, Auclair D, Taylor I, Gedrich R, Voznesensky A, Riedl B, Post LE, Bollag G and Trail PA. BAY 43-9006 exhibits broad spectrum oral antitumor activity and targets the RAF/MEK/ERK pathway and receptor tyrosine kinases involved in tumor progression and angiogenesis. Cancer Res 2004; 64: 7099-7109.

[43] Gadaleta-Caldarola G, Divella R, Mazzocca A, Infusino S, Ferraro E, Filippelli G, Daniele A, Sabba C, Abbate I and Brandi M. Sorafenib: the gold standard therapy in advanced hepatocellular carcinoma and beyond. Future Oncol 2015; 11: 2263-2266.

[44] Cheng AL, Kang YK, Chen Z, Tsao CJ, Qin S, Kim JS, Luo R, Feng J, Ye S, Yang TS, Xu J, Sun Y, Liang H, Liu J, Wang J, Tak WY, Pan H, Burock K, Zou J, Voliotis D and Guan Z. Efficacy and safety of sorafenib in patients in the Asia-Pacific region with advanced hepatocellular carcinoma: a phase III randomised, double-blind, placebo-controlled trial. Lancet Oncol 2009; 10: 25-34.

[45] Tang W, Chen Z, Zhang W, Cheng Y, Zhang B, Wu F, Wang Q, Wang S, Rong D, Reiter FP, De Toni EN and Wang X. The mechanisms of sorafenib resistance in hepatocellular carcinoma: theoretical basis and therapeutic aspects. Signal Transduct Target Ther 2020; 5: 87.

[46] Tian Y, Lei Y, Fu Y, Sun H, Wang J and Xia F. Molecular mechanisms of resistance to tyrosine kinase inhibitors associated with hepatocellular carcinoma. Curr Cancer Drug Targets 2022; 22: 454-462.

[47] Morreale FE and Walden H. Types of ubiquitin ligases. Cell 2016; 165: 248-248.e241.

[48] Wang ZW, Hu X, Ye M, Lin M, Chu M and Shen X. NEDD4 E3 ligase: functions and mechanism in human cancer. Semin Cancer Biol 2020; 67: 92-101.

[49] Tian X, Chen Y, Peng Z, Lin Q and Sun A. NEDD4 E3 ubiquitin ligases: promising biomarkers and therapeutic targets for cancer. Biochem Pharmacol 2023; 214: 115641.

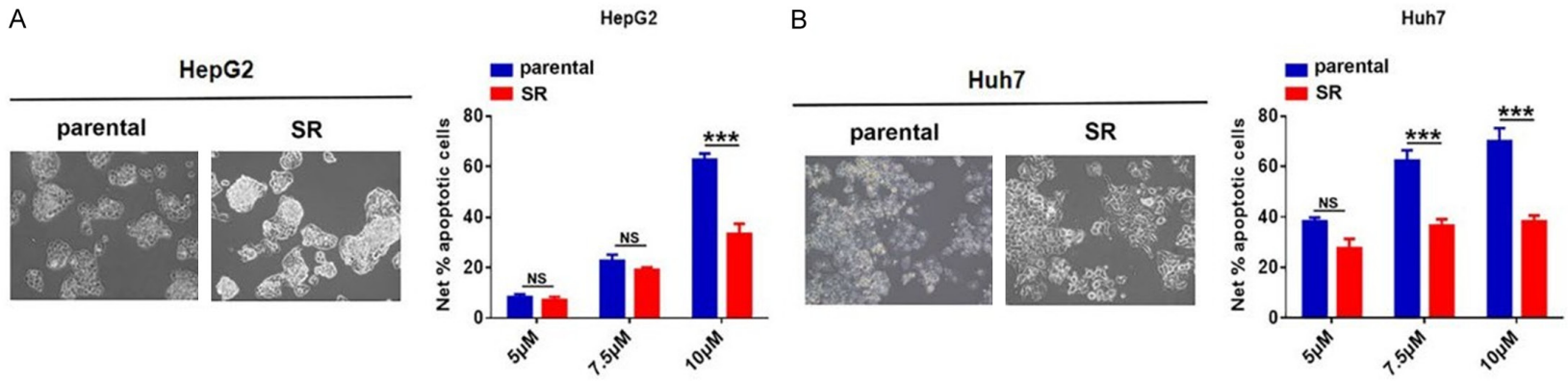

Figure S1. Differences in sorafenib sensitivity between parental and sorafenib-resistant cells. A. Bright-field images of parental and sorafenib-resistant HepG2 cells, as well as flow cytometry analysis of their apoptotic rates under different concentrations of sorafenib treatment. B. Bright-field images of parental and sorafenib-resistant Huh7 cells, as well as flow cytometry analysis of their apoptotic rates under different concentrations of sorafenib treatment. ***$P < 0.001$.

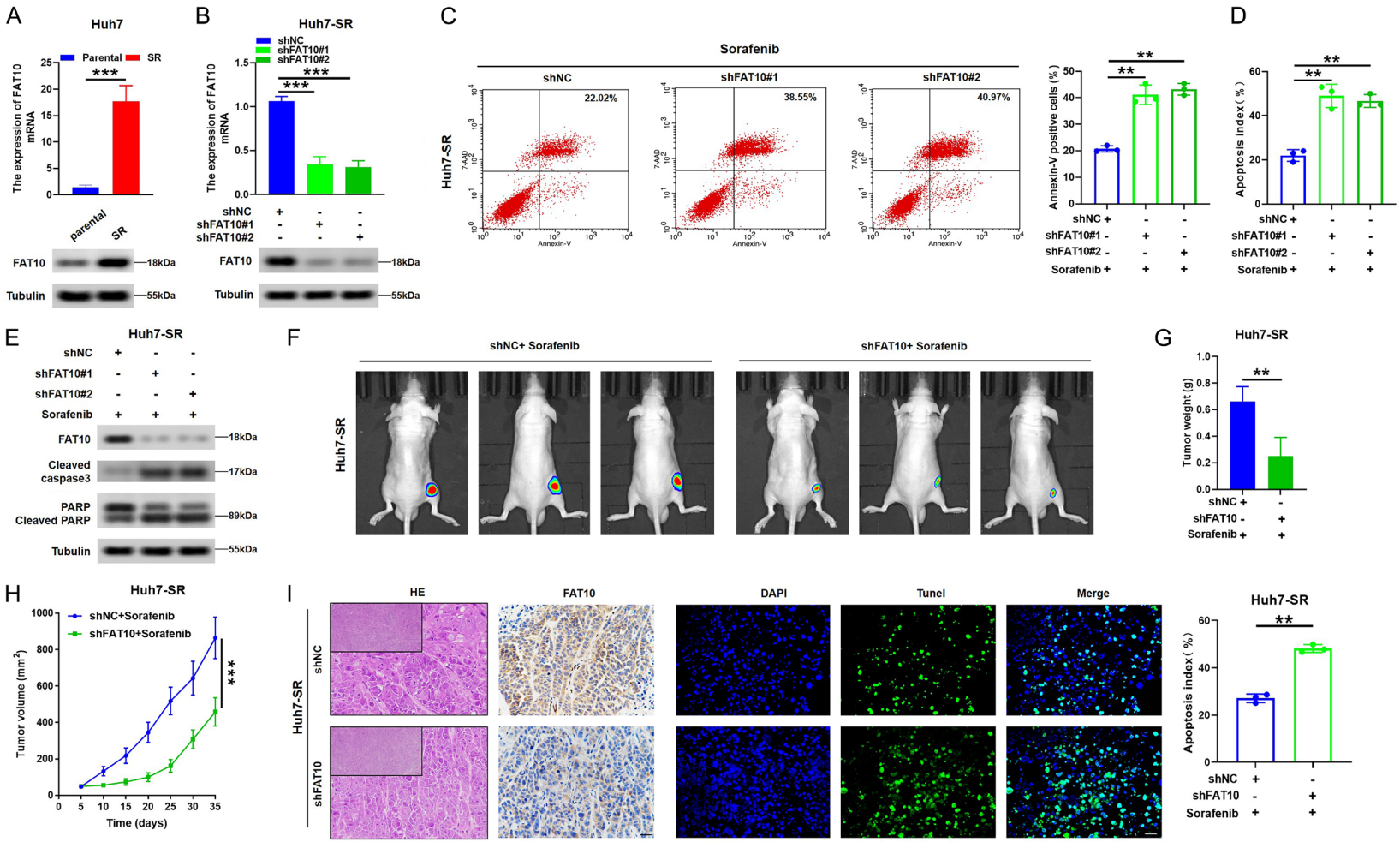

Figure S2. Reducing the expression of FAT10 in Huh7-SR cells enhances sorafenib-induced apoptosis in vitro and in vivo. (A) qRT-PCR analysis and Western blot analysis of FAT10 expression in parental and Huh7-SR cells. (B) qRT-PCR analysis and Western blot analysis of FAT10 expression in FAT10-knockdown Huh7-SR cells. (C) Flow cytometry analysis of apoptosis in shNC- or shFAT10-transfected Huh7-SR cells (7.5 μM) after exposure to sorafenib for 24 h. (D)Representative figures and quantification of TUNEL staining showing apoptotic cells (stained in green). (E) Western blot analysis of the expression of cleaved caspase, PARP, and cleaved PARP in shNC- or shFAT10-transfected Huh7-SR cells after exposure to sorafenib for 24 h. (F) Nude mice injected with luciferase-expressing shNC or shFAT10 Huh7-SR cells were treated with sorafenib (30 mg/kg/day) intraperitoneally, and then subcutaneous xenografts were assessed by an IVIS imagingsystem (n=6). (G and H) The (G) weights and (H) volumes of subcutaneous tumors were measured. (I) IHC detected the expression of FAT10 in subcutaneous xenograftsand representative figures of TUNEL staining showing apoptotic cells (stained in green) in subcutaneous xenografts. Scale bars: 100 μm. $^{**}P < 0.01$, $^{***}P < 0.001$.

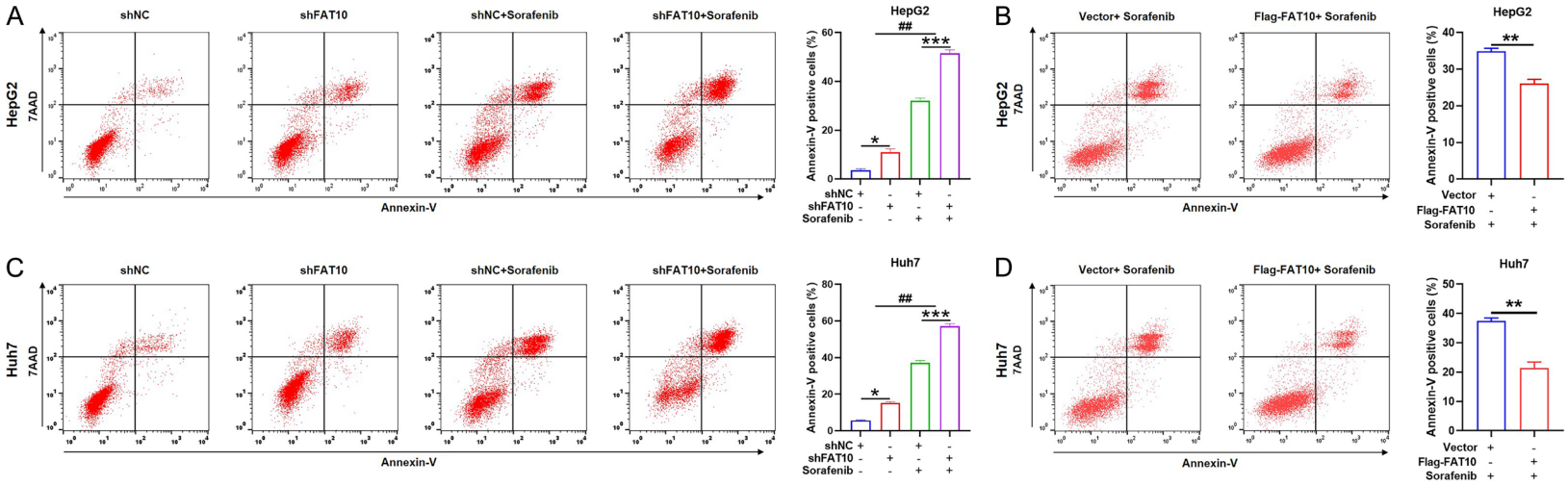

Figure S3. The effect of FAT10 expression on the sensitivity of sorafenib in HCC cells. A. Flow cytometry analysis of apoptosis in HepG2 cells with the indicated treatment. B. Flow cytometry analysis of apoptosis in Vector- or Flag-FAT10-transfected HepG2 cells after exposure to sorafenib. C. Flow cytometry analysis of apoptosis in Huh7 cells with the indicated treatment. D. Flow cytometry analysis of apoptosis in Vector- or Flag-FAT10-transfected Huh7 cells after exposure to sorafenib.

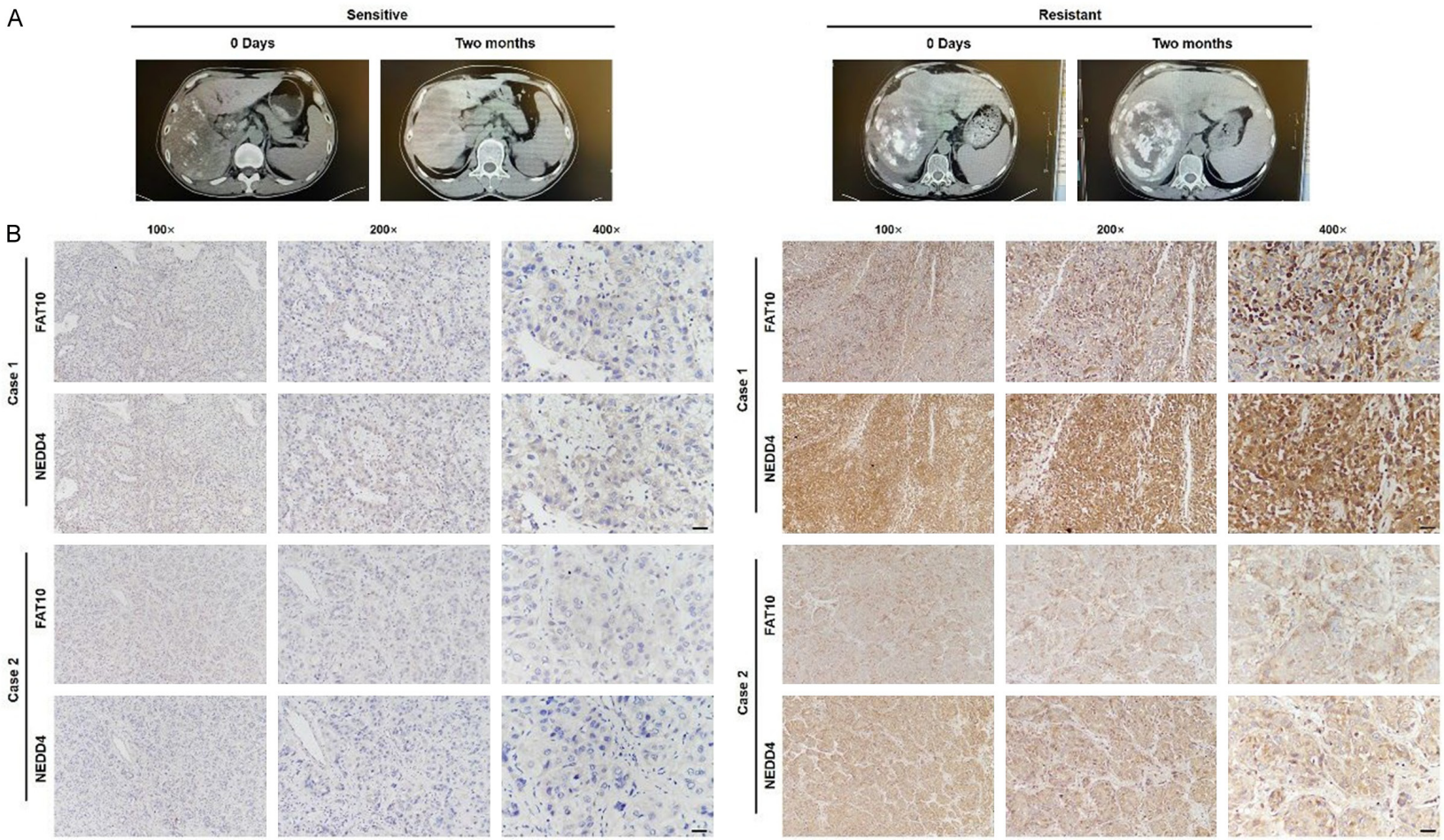

Figure S4. The expression of FAT10 and NEDD4 in sorafenib-resistant and sorafenib-sensitive HCC tissues. A. Representative radiomic features from contrast enhanced CT for patients with HCC sensitive to sorafenib before and after receiving sorafenib treatment, and IHC detected the expression of FAT10 and NEDD4 in HCC tissues sensitive to sorafenib. B. Representative radiomic features from contrast enhanced CT for patients with HCC resistant to sorafenib before and after receiving sorafenib treatment, and IHC detected the expression of FAT10 and NEDD4 in HCC tissues resistant to sorafenib. Scale bars: 100 μm.

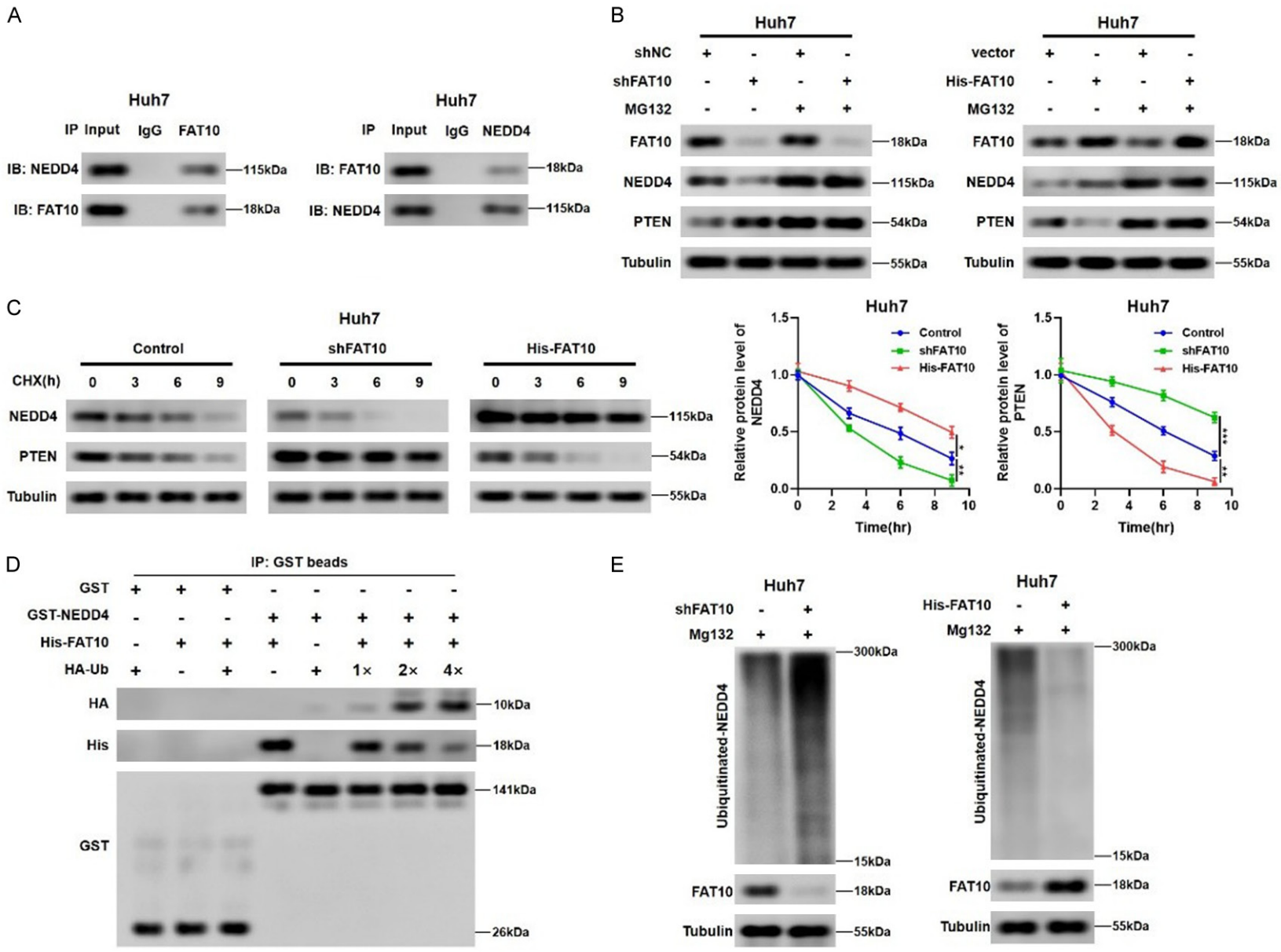
A
Huh7
IP Input IgG FAT10
IB: NEDD4
115kDa
IB: FAT10
18kDa
Huh7
IP Input IgG NEDD4
IB: FAT10
18kDa
IB: NEDD4
115kDa
B
Huh7
shNC + - + -
shFAT10 - + - +
MG132 - - + +
FAT10
18kDa
NEDD4
115kDa
PTEN
54kDa
Tubulin
55kDa
Huh7
vector + - + -
His-FAT10 - + - +
MG132 - - + +
FAT10
18kDa
NEDD4
115kDa
PTEN
54kDa
Tubulin
55kDa
C
Huh7
Control
shFAT10
His-FAT10
CHX(h) 0 3 6 9 0 3 6 9 0 3 6 9
NEDD4
PTEN
Tubulin
115kDa
54kDa
55kDa
Huh7
Relative protein level of NEDD4
Control
shFAT10
His-FAT10
Time(hr)
Huh7
Relative protein level of PTEN
Control
shFAT10
His-FAT10
Time(hr)
D
IP: GST beads
GST + + + - - - - -
GST-NEDD4 - - - + + + + +
His-FAT10 - + + + - + + +
HA-Ub + - + - + 1× 2× 4×
HA
10kDa
His
18kDa
141kDa
GST
26kDa
E
Huh7
shFAT10 - +
Mg132 + +
Ubiquitinated-NEDD4
300kDa
15kDa
FAT10
18kDa
Tubulin
55kDa
Huh7
His-FAT10 - +
Mg132 + +
Ubiquitinated-NEDD4
300kDa
15kDa
FAT10
18kDa
Tubulin
55kDa

Figure S5. FAT10 stabilizes NEDD4 expression by antagonizing its ubiquitination in Huh7 cells. A. Co-IP for FAT10 and NEDD4 in Huh7 cells. B. Western blot analysis of NEDD4 and PTEN expression in shNC- or shFAT10-transfected Huh7 cells treated with or without MG132 (15 μM). C. The cells were subjected to CHX (20 μmol/l) exposure at the indicated times, and the degradation of exogenous NEDD4 and PTEN was detected in Huh7 cells transfected with the indicated plasmids. D. Binding of NEDD4 during the course of the competition was analyzed by GST pulldown experiments. E. Huh7 cells were transfected with the indicated plasmid. The cells in each group were treated with MG132. The ubiquitination of NEDD4 was detected.

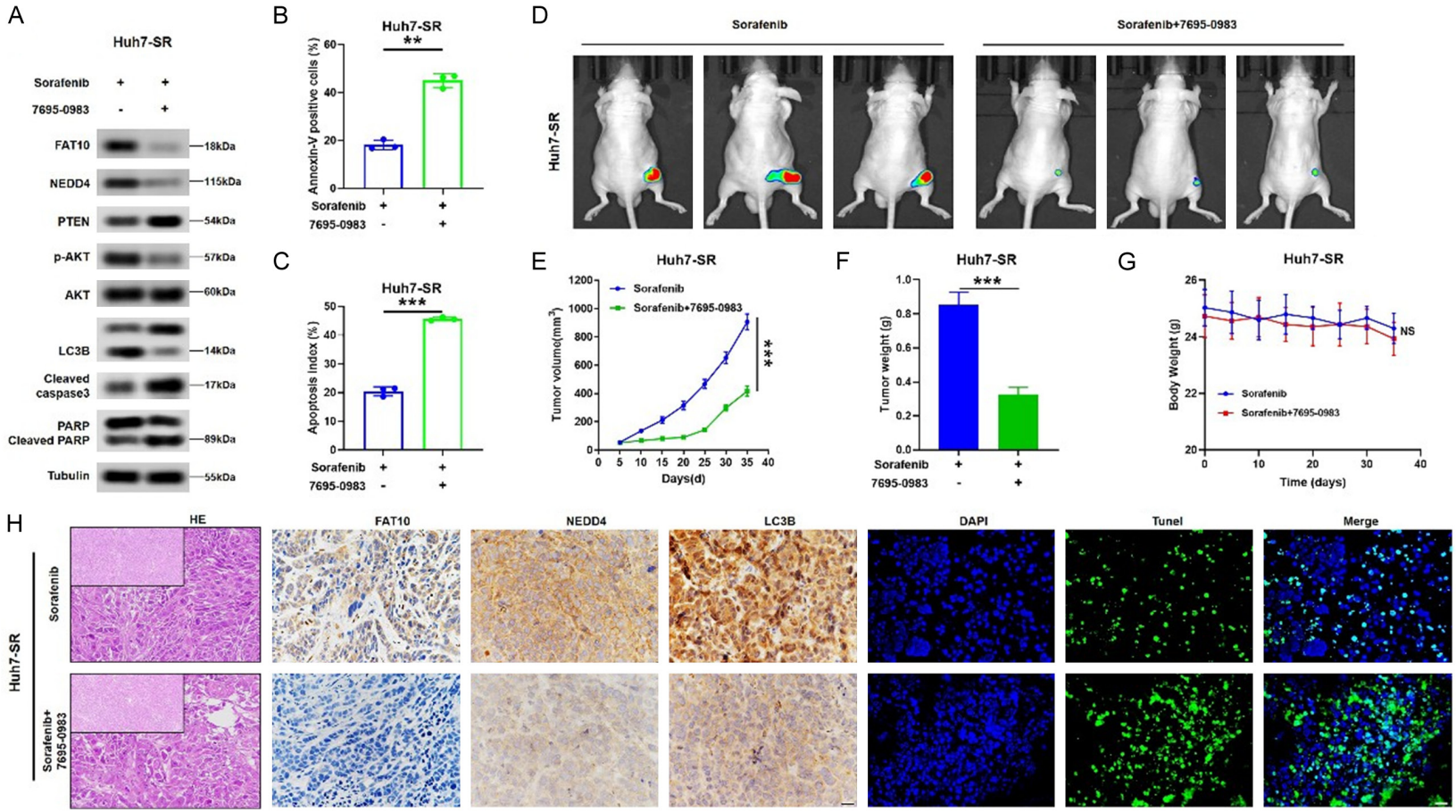

Figure S6. Targeting FAT10 inhibits the NEDD4-PTEN/AKT axis to enhance sorafenib sensitivity in Huh7-SR cells. (A) Western blot analysis of NEDD4, PTEN, AKT, p-AKT, LC3B, cleaved caspase, PARP, and cleaved PARP in Huh7-SR cells treated with sorafenib alone or combined with 7695-0983. (B and C) Flow cytometry analysis (B) and TUNEL assay (C) detection of cell apoptosis in Huh7-SR cells treated with sorafenib alone or combined with 7695-0983. (D) Nude mice injected with luciferase-expressing HepG2-SR cells and Huh7-SR cells were treated with sorafenib alone or combined with 7695-0983 intraperitoneally, and then subcutaneous xenografts were assessed by an IVIS imaging system (n=3). (E and F) The (E) volumes and (F) weights of subcutaneous tumors were measured. (G) Nude mouse body weights were recorded. (H) IHC detected the expression of FAT10, NEDD4, and LC3B in subcutaneous xenografts and representative figures of TUNEL staining showing apoptotic cells (stained in green) in subcutaneous xenografts. Scale bars: 100 μm. $^{**}P < 0.01$, $^{***}P < 0.001$.